**ÇANKAYA UNIVERSITY
GRADUATE SCHOOL OF NATURAL AND APPLIED SCIENCES
ELECTRONIC AND COMMUNICATION ENGINEERING**

MASTER THESIS

**COMPARISON OF BEAM PROFILES FROM ANALYTIC
SOLUTION AND COMPUTATIONAL MODELS**

ÖMER KEMAL ÇATMAKAŞ

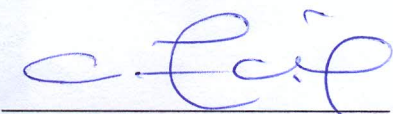**JANUARY 2014**

Title of the Thesis   : **Comparison of Beam Profiles From Analytic Solution and**
                         Computational Models

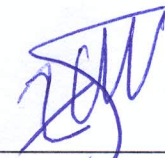Submitted by   : **Ömer Kemal ÇATMAKAŞ**

Approval of the Graduate School of Natural and Applied Sciences, Çankaya University

Prof. Dr. Taner ALTUNOK
Director

I certify that this thesis satisfies all the requirements as a thesis for the degree of Master of Science.

Prof. Dr. Celal Zaim ÇİL
Head of Department

This is to certify that we have read this thesis and that in our opinion it is fully adequate, in scope and quality, as a thesis for the degree of Master of Science.

Prof. Dr. H. Tanyer EYYUBOĞLU
Supervisor

Examination Date: 31.01.2014

Examining Committee Members:
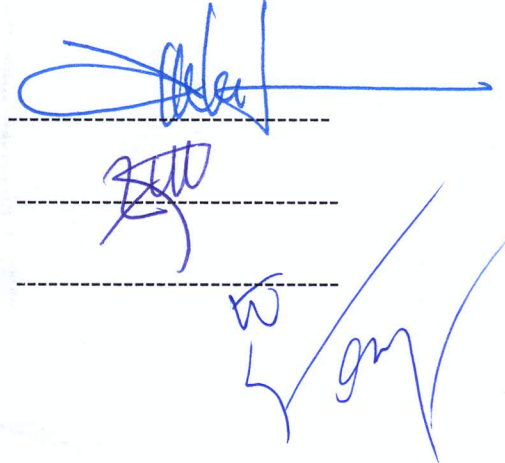
Prof. Dr. M. Önder EFE   (Hacettepe Univ.) -----------------------------

Prof. Dr. H. Tanyer EYYUBOĞLU   (Çankaya Univ.) -----------------------------

Assist. Prof. Dr. B. Uğur TÖREYİN   (Çankaya Univ.) -----------------------------

STATEMENT OF NON-PLAGIARISM

I hereby declare that all information in this document has been obtained and presented in accordance with academic rules and ethical conduct. I also declare that, as required by these rules and conduct, I have fully cited and referenced all material and results that are not original to this work.

Name, Last Name : Ömer Kemal Çatmakaş

Signature :

Date :31.01.2014

ABSTRACT

COMPARISON OF BEAM PROFILES FROM ANALYTIC SOLUTION AND COMPUTATIONAL MODELS

ÇATMAKAŞ, Ömer Kemal

M.S., Department of Electronic and Communication Engineering

Supervisor: Prof.Dr. Halil Tanyer EYYUBOĞLU

January 2014, 78 pages

In this thesis, we have compared the receiver plane beam profiles by computing the Huygens-Fresnel integral as convolution integral and Fourier integral operator and the results obtained from analytic derivation. The comparisons made on different beam types such as Gaussian, Annular-Gaussian, Sine-Gaussian, Sinh-Gaussian, Cos-Gaussian, Cosh-Gaussian beams. To make computations and comparisons we have developed a Matlab code, this code formulates the field expression for beam types on source plane, computes the receiver plane intensity distribution for three approaches of Huygens-Fresnel diffraction integral, and compares the results. Using this code, for the mentioned beam types, receiver beam profiles are computed and compared against different propagation distances and different beam parameters in free space.

Keywords: Free Space Optics, Diffraction, Angular Spectrum

ÖZ

IŞIK HÜZME PROFİLLERİNİN ANALİTİK ÇÖZÜMÜ İLE HESAPLANABİLİR MODELLERİNİN KIYASLANMASI

ÇATMAKAŞ, Ömer Kemal

Yüksek Lisans, Elektronik ve Haberleşme Anabilim Dalı

Tez Yöneticisi: Prof.Dr. Halil Tanyer EYYUBOĞLU

Ocak 2014, 78 sayfa

Bu tezde, Huygens-Fresnel entegralini, büklüm entegrali ve Fourier dönüşüm entegrali olarak hesaplayıp elde edilen ışık huzme profillerini, Huygens-Fresnel entegralinin analitik çözümünden elde edilen sonuçlarla kıyasladık . Kıyaslamalar Gaussian, Cos-Gaussian, Cosh-Gaussian, Sine-Gaussian, Sinh-Gaussian ve Annular gibi değişik ışık huzme tipleri üzerinde yapıldı. Kıyaslamaları yapmak için bir matlab kodu geliştirdik, bu kod kaynak düzlemede ışık huzmelerini oluşturabilmekte ve yoğunluklarını çizebilmekte, alıcı düzlemi için Huygens-Fresnel dağılma entegralinin her üç yaklaşımını hesaplayabilmekte, ve elde edilen sonuçları kıyaslayabilmektedir. Bu kod kullanılarak bahsi geçen ışık huzme tipleri için. alıcı düzlemde ki ışık yoğunlukları serbest uzayda, farklı yayılma mesafelerinde ve değişik huzme parametreleri ile hesaplanmış analitik çözüm ile farkları hesaplanmıştır.

Anahtar Kelimeler: Serbest Uzay Optiği, Dağılma, Açısal Spektrum

ACKNOWLEDGEMENTS

TABLE OF CONTENTS

LIST OF TABLES

LIST OF FIGURES

LIST OF ABBREVIATIONS

FSO   Free Space Optics

IR   Infrared

TEM   Transverse Electromagnetic

DFA   Difference Between Fourier Transform Integral and Analytic Solution

DCA   Difference Between Convolution Integral and Analytic Solution

CHAPTER 1

INTRODUCTION

1.1 Background Information

The concept of Free Space Optics (FSO) technology or optical wireless technology depends on transmitting modulated data by using both visible or infrared (IR) light beams. Unlike traditional communication techniques, such as, copper wire or fiber-optics which transmits laser beam into a glass fiber, FSO sends laser beams through the air.

FSO communication systems uses optical amplifiers and telescopic lens system to send and receive optical signals both on transmitter and receiver sides. Engineering task of FSO system includes not only design of these amplification or telescopic systems but also computing the propagation of light beams.

The propagation behavior of an optical wave is fundamentally governed by paraxial wave equation. Another solution for propagation of light is Huygens-Fresnel integral. Analytically solving this integral expression is difficult for many optical waves but a few simple models[1]. In this case instead of trying to solve this integral analytically, computing it as convolution integral or as Fourier integral operator which are called computational models are very sufficient methods.

1.2 Fourier Transform

Fourier transform is a mathematical operation that transforms signals between time (or spatial) and frequency domain. Fourier transform is a reversible operation. Application of Fourier transform in optics often includes 2 spatial dimensions [2] and also called angular spectrum of 2D signal. Analytic expression of Fourier transform of function g with two spatial variable x and y given in Eq. (1.1)

$$G(f_x, f_y) = \int_{-\infty}^{\infty} \int_{-\infty}^{\infty} g(x, y) e^{\left[-j2\pi\left(f_x x + f_y y\right)\right]} dx dy. \qquad (1.1)$$

where $G(f_x, f_y)$ is the transform result and f_x and f_y are independent frequency variables associated with x and y. Short notation of Fourier transform is $F\{g(x, y)\} = G(f_x, f_y)$ and $F^{-1}\{G(f_x, f_y)\} = g(x, y)$ is short notation of inverse Fourier transform, the analytic inverse Fourier transform is given in Eq. (1.2)

$$g(x, y) = \int_{-\infty}^{\infty} \int_{-\infty}^{\infty} G(f_x, f_y) e^{\left[j2\pi\left(f_x x + f_y y\right)\right]} df_x df_y. \qquad (1.2)$$

1.3 Convolution Theorem

Convolution is a mathematical operation that takes two functions of time or space and gives an output as overlapped area of these two functions while one of them is inverted according to origin and overlapping into non-inverted one, while shifting along their mutual axis. The operation of convolution is denoted with $\otimes$. Convolution integral in two dimensions is given in Eq. (1.3)

$$g(x, y) \otimes h(x, y) = \int\limits_{-\infty}^{\infty} \int\limits_{-\infty}^{\infty} g(\xi, \varsigma) h(x - \xi, y - \varsigma) d\xi d\varsigma \qquad (1.3)$$

Convolution theorem and Fourier transform have pointwise product relationship. Such that computing convolution of two functions gives the same result by taking the Fourier transform of these two functions separately then multiply them and taking the inverse Fourier transform of the result. The relationship shown in Eq. (1.4)

$$g(x, y) \otimes h(x, y) = F^{-1}\left\{ F\left\{ g(x, y) \right\} F\left\{ h(x, y) \right\} \right\}. \qquad (1.4)$$

1.4 Optical Propagation

In all FSO applications it is necessary to know the propagation characteristic of light beam. Light has both particle and wave properties. Particle like properties of light are emission, absorption etc., wave like properties of light are propagation, interference, diffraction etc. In free space light propagates with a constant speed which denoted as "c" and the value of c is approximately $3x10^8$ m/s. The range of optical wavelength domain starts from 10 nm and extends up to 1 mm. This domain includes three bands which are Ultraviolet(10nm to 390 nm), Visible(390nm to 760nm), and Infrared(760nm to 1mm) [3]. Electromagnetic spectrum [4] given in figure 1.1.
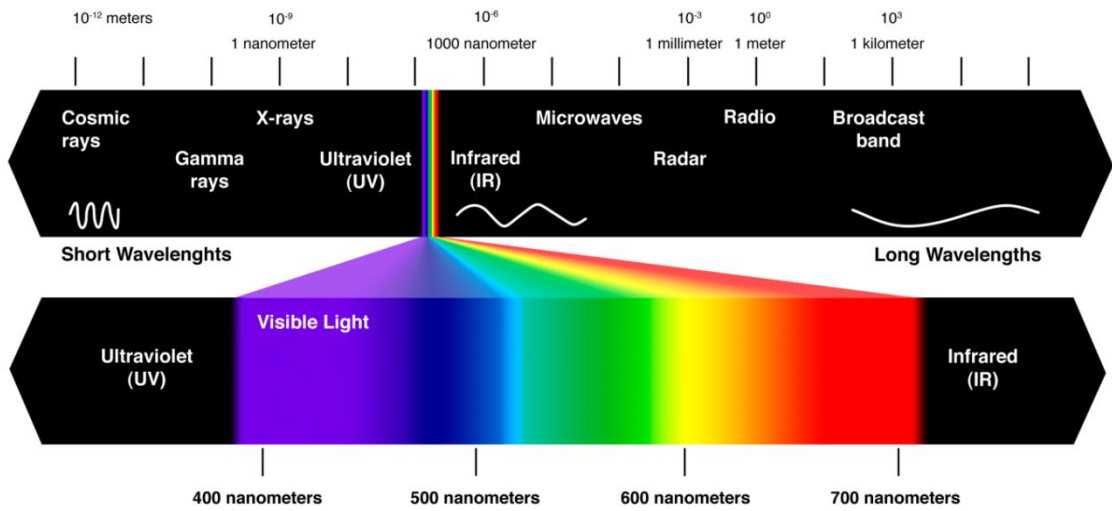
Figure 1.1 Electromagnetic Spectrum

Propagation can be defined as relocation of an optical field from one position to another. An optical field denoted by $u(r,t)$ which is a function of position $r = (x, y, z)$ and time t. This field mathematically satisfies the wave equation which is given in Eq.(1.5)

$$\nabla^2 u = \frac{1}{c^2} \frac{\partial^2 u}{\partial t^2}$$

(1.5)

where c is the speed of light and ∇^2 represents the Laplacian operator. In rectangular coordinates Laplacian operator defined in Eq. (1.6)

$$\nabla^2 u = \frac{\partial^2 u}{\partial x^2} + \frac{\partial^2 u}{\partial y^2} + \frac{\partial^2 u}{\partial z^2}$$

(1.6)

4

If the time variations in the optical field is harmonic(i.e. Sinusoidal) $u(r,t)$ can be denoted in the form $u(r,t) = u(r)e^{-j\omega t}$, where ω is the angular frequency, $j = \sqrt{-1}$ and $u(r)$ is the complex amplitude of wave, and Eq. (1.5) can be reduced into time independent form of wave equation which is called Helmholtz Equation and shown in Eq. (1.7)

$$\nabla^2 u + k^2 u = 0 \tag{1.7}$$

If we consider propagation is nearly parallel to the axis z, we can write the time independent optical field as in Eq. (1.8)

$$u(x, y, z = L) = u_r(r_x, r_y)e^{-jkL} \tag{1.8}$$

where k is the wave number and λ is optical wavelength which is $\lambda = 2\pi / k$. Substituting (1.8) into Helmholtz's Eq. (1.7) we obtain Eq. (1.9)

$$\left[\frac{\partial^2 u_r}{\partial x^2} + \frac{\partial^2 u_r}{\partial y^2} + \frac{\partial^2 u_r}{\partial z^2} + 2jk\frac{\partial u_r}{\partial z} - k^2 u_r \right] e^{-jkL} + k^2 u_r e^{-jkL} = 0 \tag{1.9}$$

The paraxial approximation neglects $\partial^2 u_r / \partial z^2$ since u_r is assumed to vary slowly with z, and cancels e^{-jkL} term. This yields the paraxial wave equation [5], shown in Eq. (1.10)

$$\frac{\partial^2 u_r}{\partial x^2} + \frac{\partial^2 u_r}{\partial y^2} + 2jk\frac{\partial u_r}{\partial z} = 0 \tag{1.10}$$

Solving paraxial wave equation is very easy by computing its two dimensional Fourier transform. Let Fourier transform of $u_r(x, y)$ be $U_r(f_x, f_y)$, and since

$F\left(\dfrac{d^n f(x)}{dx^n}\right) = (2\pi j f_x)^n F(f_x)$ Eq. (1.10) transforms into Eq. (1.11)

$$(j2\pi f_x)^2 U_r + (j2\pi f_y)^2 U_r + 2jk\frac{\partial U_r}{\partial z} = 0 \tag{1.11}$$

After arrangement of Eq. (1.11) we obtain Eq. (1.12);

$$\frac{\partial U_r}{\partial z} = \left(\frac{2\pi^2}{jk}\right)(f_x^2 + f_y^2)U_r \tag{1.12}$$

Eq. (1.12) may be integrated directly;

$$U_r(f_x, f_y) = U_s(f_x, f_y)e^{\left[\frac{2\pi^2}{jk}\left(f_x^2 + f_y^2\right)L\right]} \tag{1.13}$$

since the inverse Fourier transform of $e^{\left[\frac{2\pi^2}{jk}\left(f_x^2 + f_y^2\right)L\right]}$ is $h(r_x, r_y) = \dfrac{1}{j\lambda L}e^{\left[\frac{jk}{2L}\left(r_x^2 + r_y^2\right)\right]}$ [6] we

can obtain the inverse Fourier transform (1.13) by the help of convolution relationship (1.14a), and Eq. (1.14b) is the convolution in full form.

$$u_z(r_x, r_y) = u_s \otimes h(r_x, r_y) \tag{1.14a}$$

$$u_r\left(r_x, r_y\right) = \frac{1}{j\lambda L} \int\limits_{-\infty}^{\infty}\int\limits_{-\infty}^{\infty} u_s\left(s_x, s_y\right) e^{\left[\frac{jk}{2L}\left(\left(r_x - s_x\right)^2 + \left(r_y - s_y\right)^2\right)\right]} ds_x ds_y \qquad (1.14b)$$

Eq. (1.14b) is called the paraxial diffraction integral, solution of this integral for a given field u_s at L=0 as source plane with coordinates $\left(s_x, s_y\right)$ gives (u_r) at L distance away with receiver coordinates of $\left(r_x, r_y\right)$. Whenever this integral is valid, the receiver plane is said to be in the Fresnel Region. Huygens-Fresnel approximation of this integral adds back e^{-jkL} term to both sides, adding this term we get Huygens-Fresnel integral, at Eq. (1.15) and Free space propagation geometry is given in Figure 1.2 [17]

$$u_r\left(r_x, r_y, L\right) = \frac{-jke^{-jkL}}{2\pi L} \int\limits_{-\infty}^{\infty}\int\limits_{-\infty}^{\infty} u_s\left(s_x, s_y\right) e^{\left[\frac{jk}{2z}\left(\left(r_x - s_x\right)^2 + \left(r_y - s_y\right)^2\right)\right]} ds_x ds_y \qquad (1.15)$$
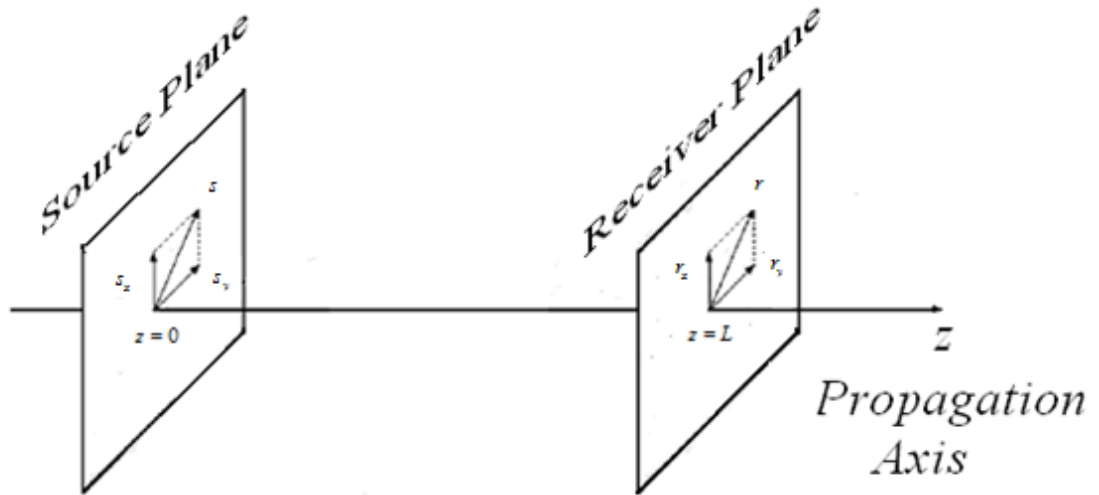
Figure 1.2 Propagation Geometry

CHAPTER 2

METHODS AND EXPERIMENTS

2.1 Gaussian Beam Optics

In most optical applications, lasers emit beams with a Gaussian profile. The Gaussian beam is a Transverse Electromagnetic(TEM) mode wave [7]. Gaussian beam waves mostly used in lowest order transverse electromagnetic mode in the other words fundamental transverse mode and it is denoted by TEM_{00}.

For theoretical study of optical wave propagation, Gaussian beam is more sufficient than plane wave or spherical wave when focusing and diverging parameters are important[8]. At a propagation distance L, lowest order transverse electromagnetic wave Gaussian beam wave formulation [9] in cylindrical coordinates with amplitude coefficient A_c is given in Eq. (2.1)

$$u(r,\phi,L) = \frac{A_c}{1+2j\alpha L} \exp\left(\frac{-k\alpha r^2}{1+2j\alpha L}\right) \exp\left(jkL\right) \tag{2.1}$$

On source plane (at L=0) Gaussian source field can expressed in Eq. (2.2);

$$u_s(s, \phi_s, L = 0) = A_c \exp(-k\alpha s^2) \tag{2.2}$$

where $\alpha = \dfrac{1}{kW_s^2} + \dfrac{j}{2F_s}$, W_s (in m) refers to radial Gaussian source size (beam waist) and F_s refers to focusing parameter. Beam waist (W_s) denotes when the radius is equal to $1/e$ as shown in fig. (2-1)
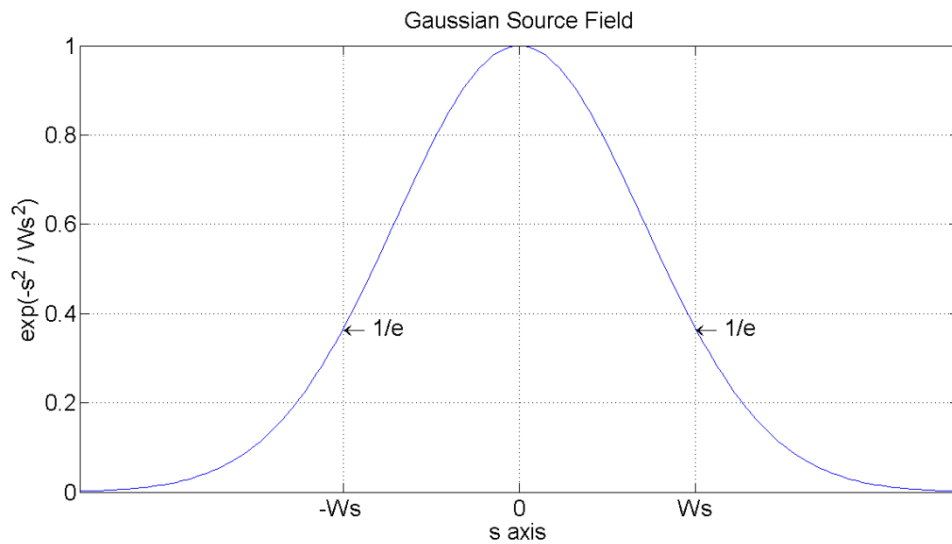
Figure 2-1 Amplitude profile of a Gaussian beam.

Travelling Gaussian beam in Eq. (2.1) is a solution for paraxial wave equation [3], for propagation of an optical field, another solution is called Huygens-Fresnel integral. With the help of this integral, it is possible to find the received field from a given source field. For inconvenience in Eq. (2.3a) and Eq. (2.3b) the expression of this integrals are given respectively for cylindrical and Cartesian coordinates.

$$u_r(r,\phi_r,L) = \frac{-jk\exp(jkL)}{2\pi L} \int\limits_{-\infty}^{\infty}\int\limits_{-\infty}^{\infty} ds\, d\phi_s u_s(s,\phi_s)\exp\left[\frac{jk}{2L}\left[-2rs\cos(\phi_r-\phi_s)+s^2+r^2\right]\right] \quad (2.3a)$$

$$u_r(\mathbf{r},L) = \frac{-jk\exp(jkL)}{2\pi L} \int\limits_{-\infty}^{\infty}\int\limits_{-\infty}^{\infty} d^2s\, u_s(\mathbf{s})\exp\left[\frac{jk}{2L}(\mathbf{r}-\mathbf{s})^2\right]$$

$$\text{with} \quad \mathbf{s}=(s_x,s_y) \quad, \quad \mathbf{r}=(r_x,r_y)$$

$$u_r(r_x,r_y,L) = \frac{-jk\exp(jkL)}{2\pi L} \int\limits_{-\infty}^{\infty}\int\limits_{-\infty}^{\infty} ds_x ds_y u_s(s_x,s_y)\exp\left\{\frac{jk}{2L}\left[(r_x-s_x)^2+(r_y-s_y)^2\right]\right\} \quad (2.3b)$$

$$= \frac{-jk\exp(jkL)}{2\pi L} \int\limits_{-\infty}^{\infty}\int\limits_{-\infty}^{\infty} ds_x ds_y u_s(s_x,s_y)$$

$$\exp\left\{\frac{jk}{2L}\left[-2s_x r_x -2s_y r_y + s_x^2 + s_y^2 + r_x^2 + r_y^2\right]\right\}$$

2.2 Computing Huygens-Fresnel Integral as Fourier Integral and Convolution Integral

Huygens-Fresnel integral in Cartesian coordinates is given in Eq. (2.3b). To obtain Fourier transform integral from Fresnel diffraction integral, the last exponential term need to be splitted as shown in Eq. (2.4).

$$u_r(r_x,r_y,L) = \frac{-jk\exp(jkL)}{2\pi L}\exp\left[\frac{jk}{2L}(r_x^2+r_y^2)\right]$$

$$\int\limits_{-\infty}^{\infty}\int\limits_{-\infty}^{\infty} ds_x ds_y u_s(s_x,s_y)\exp\left[\frac{jk}{2L}(s_x^2+s_y^2)\right]\exp\left[\frac{-jk}{L}(s_x r_x + s_y r_y)\right] \quad (2.4)$$

If the Eq. (2.4) is analyzed, it is seen that, there is a Fourier transform relationship between s (source)and r (receiver) planes . The last exponential term in Eq. (2.4) behaves like Fourier integral operator and can expressed like in Eq. (2.5);

$$u_r\left(r_x, r_y, L\right) = \frac{-jk\exp\left(jkL\right)}{2\pi L}\exp\left[\frac{jk}{2L}(r_x^2 + r_y^2)\right]F\left\{u_s\left(s_x, s_y\right)\exp\left[\frac{jk}{2L}(s_x^2 + s_y^2)\right]\right\} \qquad (2.5)$$

where $F\{\}$ indicates the Fourier transform operator in Eq. (2.5). Direct application of this form of the integral in propagation simulation is possible if and only if coordinates of source and receiver plane are identical [10]. Otherwise a scaling parameter between source and receiver plane need to be integrated into formulation. To introduce the scaling parameter it is needed to go back to Eq. (2.4) and that $r = m_f s$ where r and s respectively indicates receiver and source plane coordinates and m_f is multiplying factor. Tyler and Fried [11] discussed how to approach the scaling parameter, and using their approach we can rearrange the exponential and with the introduction of this scaling term $(\mathbf{r} - \mathbf{s})^2$ inside the diffraction exponential will become in Eq. (2.6);

$$(\mathbf{r} - \mathbf{s})^2 = m_f\left(\frac{\mathbf{r}}{m_f} - \mathbf{s}\right)^2 - \left(\frac{1 - m_f}{m_f}\right)\mathbf{r}^2 + (1 - mf)\mathbf{s}^2 \qquad (2.6)$$

Inserting Eq. (2.6) into Eq. (2.4) we get Eq. (2.7a) and Eq. (2.7b)

$$u_r(\mathbf{r}, L) = \frac{-jk\exp\left(jkL\right)}{2\pi L}\int_{-\infty}^{\infty}\int_{-\infty}^{\infty} d^2 s u_s(s)$$
$$\exp\left[\frac{jk}{2L}\left(m_f\left(\frac{\mathbf{r}}{m_f} - \mathbf{s}\right)^2 - \left(\frac{1 - m_f}{m_f}\right)\mathbf{r}^2 + (1 - mf)\mathbf{s}^2\right)\right] \qquad (2.7a)$$

$$u_r(\mathbf{r}, L) = \frac{-jk\exp\ jkL}{2\pi L}\exp\left[\frac{jk}{2L}\left(\frac{1 - m_f}{m_f}\right)\mathbf{r}^2\right]\int_{-\infty}^{\infty}\int_{-\infty}^{\infty} d^2 s u_s(s)$$
$$\exp\left[\frac{jk}{2L}m_f\left(\frac{\mathbf{r}}{m_f} - \mathbf{s}\right)^2\right]\exp\left[\frac{jk}{2L}(1 - mf)\mathbf{s}^2\right] \qquad (2.7b)$$

By introducing Eq. (2.8)

$$u_{s1}(\mathbf{s}) = \frac{1}{m_f} u_s(\mathbf{s}) \exp\left[\frac{jk}{2L}(1-m_f)\mathbf{s}^2\right] \tag{2.8}$$

Eq. (2.7b) turns into Eq. (2.9)

$$u_r(\mathbf{r}, L) = \frac{-jkm_f \exp jkL}{2\pi L} \exp\left[\frac{jk}{2L}\left(\frac{1-m_f}{m_f}\right)\mathbf{r}^2\right] \int_{-\infty}^{\infty}\int_{-\infty}^{\infty} d^2s u_{s1} \; \mathbf{s} \; \exp\left[\frac{jk}{2L}m_f\left(\frac{\mathbf{r}}{m_f}-\mathbf{s}\right)^2\right] \tag{2.9}$$

Now by introducing and applying new scaling terms $\mathbf{r_1} = \mathbf{r}/m_f$, $L_1 = L/m_f$,Eq. (2.9) will become Eq. (2.10);

$$u_r(\mathbf{r}, L) = \frac{-jk \exp jkL}{2\pi L_1} \exp\left[\frac{jk}{2L}\left(\frac{1-m_f}{m_f}\right)\mathbf{r}^2\right] \int_{-\infty}^{\infty}\int_{-\infty}^{\infty} d^2s m u_{s1}(\mathbf{s}) \exp\left[\frac{jk}{2L_1}(\mathbf{r_1}-\mathbf{s})^2\right] \tag{2.10}$$

Eq. (2.10) is in the form of convolution integral as written in Eq. (2.11);

$$u_r(\mathbf{r}, L) = \exp(jkL)\exp\left[\frac{jk}{2L}\left(\frac{1-m_f}{m_f}\right)\mathbf{r}^2\right] \int_{-\infty}^{\infty}\int_{-\infty}^{\infty} d^2s u_{s1}(\mathbf{s}) \; h(\mathbf{r_1}-\mathbf{s}) \tag{2.11}$$

where the transfer function $h(\mathbf{r_1}-\mathbf{s})$ is in Eq. (2.12);

$$h(\mathbf{r}_1 - \mathbf{s}) = \frac{-jk}{2\pi L_1} \exp\left[\frac{jk}{2L_1}(\mathbf{r}_1 - \mathbf{s})^2\right] \qquad (2.12)$$

Taking the Fourier transform of transfer function, we get Eq. (2.13)

$$H(\mathbf{f}) = \mathbf{F}\left[h(\mathbf{r}_1 - \mathbf{s})\right] = \exp\left(-j\pi\lambda L_1 \mathbf{f}^2\right) = \exp\left(-j\pi\lambda \frac{L}{m_f}\mathbf{f}^2\right) = \exp\left(-\frac{2j\pi^2 L}{m_f k}\mathbf{f}^2\right) \qquad (2.13)$$

Finally Huygens-Fresnel integral can be shown as in Eq. (2.14);

$$u_r(\mathbf{r}, L) = \exp(jkL)\exp\left[\frac{jk}{2L}\left(\frac{1-m_f}{m_f}\right)\mathbf{r}^2\right] u_{s1}(\mathbf{s}) \otimes h(\mathbf{r}_1) \qquad (2.14)$$

With help of the pointwise product relationship of Eq. (2.14) will become as shown in Eq. (2.15a), Eq. (2.15b), and Eq. (2.15c)

$$u_r(\mathbf{r}, L) = \exp(jkL)\exp\left[\frac{jk}{2L}\left(\frac{1-m_f}{m_f}\right)\mathbf{r}^2\right] \mathbf{F}^{-1}\left\{\mathbf{F}\left[u_{s1}(\mathbf{s})\right]\mathbf{F}\left[h(\mathbf{r}_1)\right]\right\} \qquad (2.15a)$$

$$u_r(\mathbf{r}, L) = \exp(jkL)\exp\left[\frac{jk}{2L}\left(\frac{1-m_f}{m_f}\right)\mathbf{r}^2\right] \mathbf{F}^{-1}\left\{\mathbf{F}\left[u_{s1}(\mathbf{s})\right]H(\mathbf{f})\right\} \qquad (2.15b)$$

$$u_r(\mathbf{r}, L) = \exp(jkL)\exp\left[\frac{jk}{2L}\left(\frac{1-m_f}{m_f}\right)\mathbf{r}^2\right]$$
$$\mathbf{F}^{-1}\left\{\mathbf{F}\left[u_s(\mathbf{s})\frac{1}{m_f}\exp\left[\frac{jk}{2L}(1-m_f)s^2\right]\right]H(\mathbf{f})\right\} \qquad (2.15c)$$

2.3 Beam Types

In this thesis we make comparisons among Gaussian beam, Cos-Gaussian beam, Cosh-Gaussian beam, Sine-Gaussian beam, Sinh-Gaussian beam, Annular Gaussian beam, and we chose these beams because of their analytic solutions are already obtained. Eq. (2.16) is used to obtain the different beam types on source plane[12-13] and Eq. (2.17) is the analytical expression of propagated beams on receiver plane[13-14-15] .

$$u_s(s_x, s_y) = \sum_{\ell=1}^{2} A_\ell \exp\left[-0.5k(\alpha_{x\ell}s_x^2 + \alpha_{y\ell}s_y^2) + D_{x\ell}s_x + D_{y\ell}s_y\right] \tag{2.16}$$

$$u_r\ r_x, r_y, L = \exp\ jkL \sum_{\ell=1}^{2} \frac{A_\ell}{1 + j\alpha_{x\ell}L\ ^{0.5}\ 1 + j\alpha_{y\ell}L\ ^{0.5}} \exp\left(-\frac{0.5k\alpha_{x\ell}r_x^2}{1 + j\alpha_{x\ell}L}\right)\exp\left(\frac{D_{x\ell}r_x}{1 + j\alpha_{x\ell}L}\right)$$

$$\exp\left(\frac{0.5jD_{x\ell}^2 L}{k(1 + j\alpha_{x\ell}L)}\right)\exp\left(-\frac{0.5k\alpha_{y\ell}r_y^2}{1 + j\alpha_{y\ell}L}\right)$$

$$\exp\left(\frac{D_{y\ell}r_x}{1 + j\alpha_{y\ell}L}\right)\exp\left(\frac{0.5jD_{y\ell}^2 L}{k(1 + j\alpha_{y\ell}L)}\right) \tag{2.17}$$

Table 2.1 Parameters for different beam types

Beam Type / Parameter	Displacement Parameter 1	Displacement Parameter 2	Amplitude Coefficient	Beam Waist
Gaussian Beam	$(0,0)$	$(0,0)$	$(A_{C1},0)$	$(Ws,0)$
Cos-Gaussian Beam	$(-jD_1,-jD_1)$	(jD_2,jD_2)	(A_{C1},A_{C2})	$(Ws_1=Ws_2)$
Cosh-Gaussian Beam	(D_1,D_1)	$(-D_2,-D_2)$	(A_{C1},A_{C2})	$(Ws_1=Ws_2)$
Sine-Gaussian Beam	$(-jD_1,-j*D_1)$	(jD_2,jD_2)	$(jA_{C1},-jA_{C2})$	$(Ws_1=Ws_2)$
Sinh-Gaussian Beam	$(-D_1,-D_1)$	(D_2,D_2)	$(A_{C1},-A_{C2})$	$(Ws_1=Ws_2)$
Annular Gaussian Beam	$(0,0)$	$(0,0)$	$(A_{C1},-A_{C2})$	$(Ws_1>Ws_2)$

where $D_1 = D_{x1} = D_{y1}$, $D_2 = D_{x2} = D_{y2}$, and A_{C1}, A_{C2}, D_1, D_2 are positive quantities.

2.4 Optical Intensity

The optical intensity I(r) is defined as the optical power per unit area units of watt/m^2 is given in Eq. (2.18)

$$I(r) = u(r)u*(r) \tag{2.18}$$

where * denotes complex conjugate.

2.5 Comparison Technique

To make comparisons firstly received beam profiles are normalized with respect to received intensity of analytical solution. Then two received beam intensities are subtracted from each other along the number of grid spaces element by element and absolute difference is summed. Finally this sum is divided by square of grid spaces and multiplied with 100 to have percentage of difference. Comparison method is shown in Eq. (2.19), this method is a similar form of the one used in [16]

$$D = 100 \sum_{r_x=0, r_y=0}^{N} abs\left[I_{rcm}\left(r_x, r_y\right) - I_{ras}\left(r_x, r_y\right) \right] / \left[N^2 \max\left(\max\left(I_{ras}\left(r_x, r_y\right)\right)\right) \right] \qquad (2.19)$$

where N is the number of grids, I_{rcm} is received intensity from computational models and I_{ras} is received intensity from analytic solution.

2.6 Computing Multiplying Factor

Correct multiplication factor is achieved by demanding the power of beam on different observation (receiver) planes remain the same as source beam power. For the propagation distances lower than 500 m multiplication factor is taken as unity. For propagation distances beyond 500 m, multiplication factor is set to L/500. To calculate power of beam Eq. (2.20) formula is used.

$$P = \sum_{r_x=-N/2}^{N/2} \sum_{r_y=-N/2}^{N/2} I_{rcm}\left(r_x, r_y\right) / N^2 \qquad (2.20)$$

2.7 Sample Comparisons

2.7.1 Gaussian Beam

Fig. (2-2) shows the intensity distribution of Gaussian beam on the source plane and the receiver plane. Receiver plane intensity distributions obtained respectively by analytic expression, Fourier integral operator and convolution integral. The propagation distance between source and receiver plane is L=2 km . Multiplying factor is $m_f = 4$. The Gaussian beam parameters are $\lambda = 1.55 \mu m$, $W_{s1} = W_s = 1 cm$, $A_{c1} = 1$, $A_{c2} = 0$.

Figure 2-2 Intensity distributions of Gaussian beam .

Total received intensity difference between analytic expression and Fourier integral operator is 8.5502×10^{-6} %, difference between analytic expression and convolution integral is 0.1105 %. Fig. (2-3) shows the difference between the received beam intensities which are obtained from analytic expression and Fourier integral operator.

Figure 2-3 Received intensity difference of Gaussian beam between analytic expression and
Fourier integral operation .

Fig. (2-4) shows the difference between the received beam intensities which are
obtained from analytic expression and convolution integral.

Figure. 2-4 Received intensity difference of Gaussian beam between analytic expression and
Convolution integral.

2.7.2 Cos-Gaussian Beam

Fig. (2-5) shows the intensity distribution of Cos-Gaussian beam on the source plane and the receiver plane. Receiver plane intensity distributions obtained respectively by analytic expression, Fourier integral operator and convolution integral. The propagation distance between source and receiver plane is L=2 km . Multiplying factor is $m_f = 4$. The beam parameters are $\lambda = 1.55 \mu m$, $W_{s1} = W_{s2} = 1cm$, $Ac_1 = 0.5$, $Ac_2 = 0.5$, $D_{x1} = D_{y1} = -j200m^{-1}$, $D_{x2} = D_{y2} = j200m^{-1}$

Figure 2-5 Intensity distributions of Cos-Gaussian beam.

Total received intensity difference between analytic expression and Fourier integral operator is 0.0481 %, difference between analytic expression and convolution integral is 1.1669 %. Fig. (2-6) shows the difference between the received beam intensities which are obtained from analytic expression and Fourier integral operator.

Figure 2-6 Received intensity difference of cos-Gaussian beam between analytic expression and Fourier integral operation .

Fig. (2-7) shows the difference between the received beam intensities which are obtained from analytic expression and Fourier integral operator.

Figure 2-7 Received intensity difference of Cos-Gaussian beam between analytic expression and convolution integral.

2.7.3 Cosh-Gaussian Beam

Fig. (2-8) shows the intensity distribution of Cosh-Gaussian beam on source plane and receiver plane. Receiver plane intensity distributions obtained respectively by analytic expression, Fourier integral operator and convolution integral. The propagation distance between source and receiver plane is L=2 km . Multiplying factor is $m_f = 4$. The Gaussian beam parameters are $\lambda = 1.55\mu m$, $W_{s1} = W_{s2} = 1cm$, $A_{c1} = 0.5$, $A_{c2} = 0.5$, $D_{x1} = D_{y1} = 200m^{-1}$, $D_{x2} = D_{y2} = -200m^{-1}$
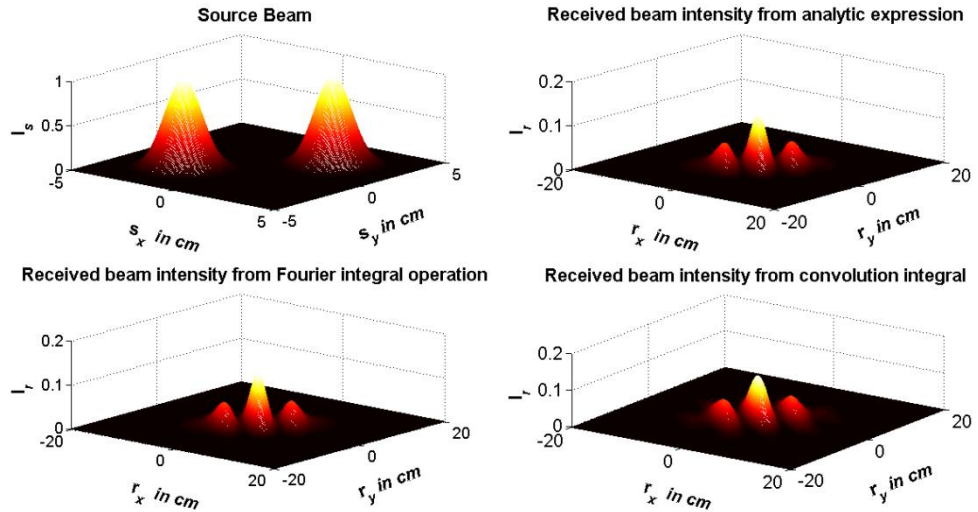
Figure 2-8 Intensity distributions of Cosh-Gaussian beam.

Total received intensity difference between analytic expression and Fourier integral operator is 0.0134 %, difference between analytic expression and convolution integral is 0.4084 %. Fig. (2-9) shows the difference between the received beam intensities which are obtained from analytic expression and Fourier integral operator.

Figure 2-9 Received intensity difference of Cosh-Gaussian beam between analytic expression and Fourier integral operator .

Fig. (2-10) shows the difference between the received beam intensities which are obtained from analytic expression and Fourier integral operator.
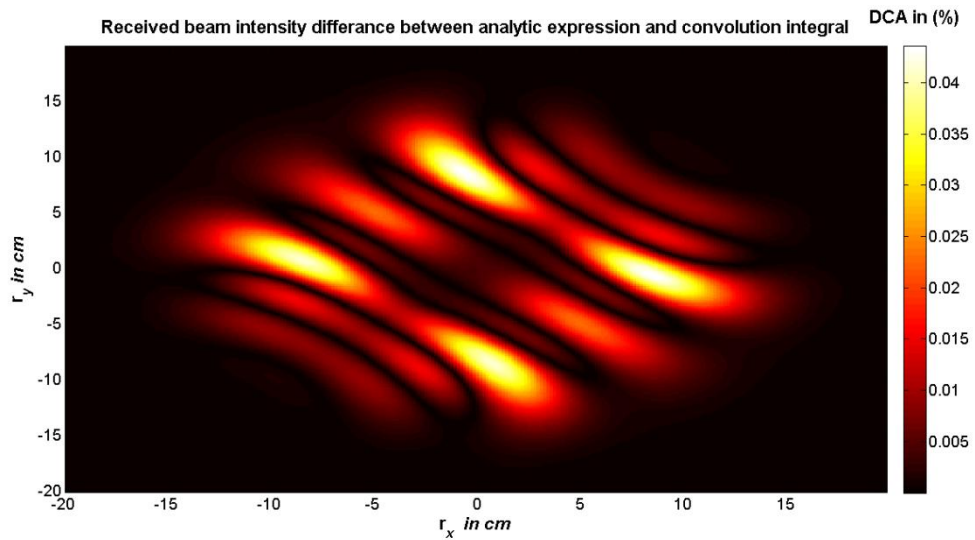
Figure 2-10 Received intensity difference of Cosh-Gaussian beam between analytic expression and convolution integral.

2.7.4 Sine-Gaussian Beam

Fig. (2-11) shows the intensity distribution of Sine-Gaussian beam on source plane and receiver plane. Receiver plane intensity distributions obtained respectively by analytic expression, Fourier integral operator and convolution integral. The propagation distance between source and receiver plane is L=2 km . Multiplying factor is $m_f = 4$. The Gaussian beam parameters are $\lambda = 1.55 \mu m$, $W_{s1} = W_{s2} = 1cm$, $A_{c1} = 0.5j$, $A_{c2} = -0.5j$, $D_{x1} = D_{y1} = -j200m^{-1}$, $D_{x2} = D_{y2} = j200m^{-1}$
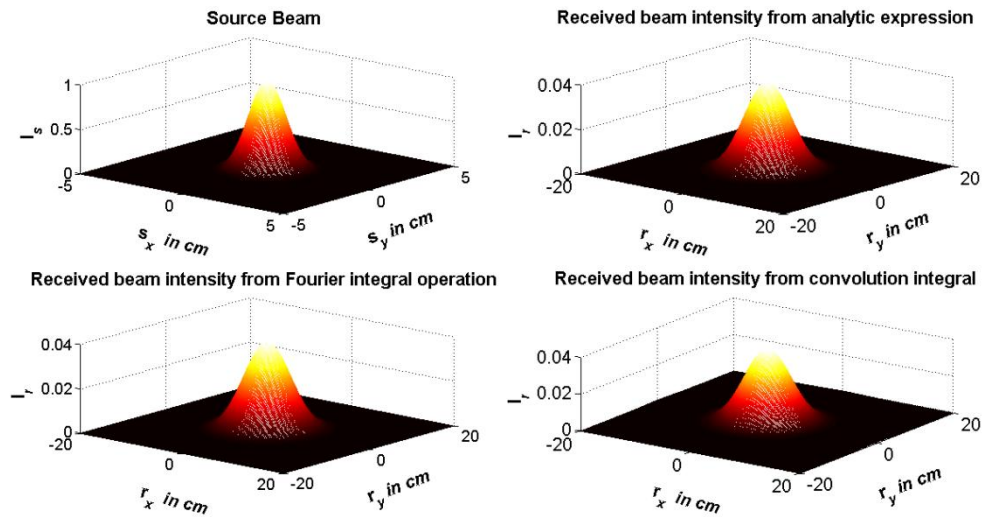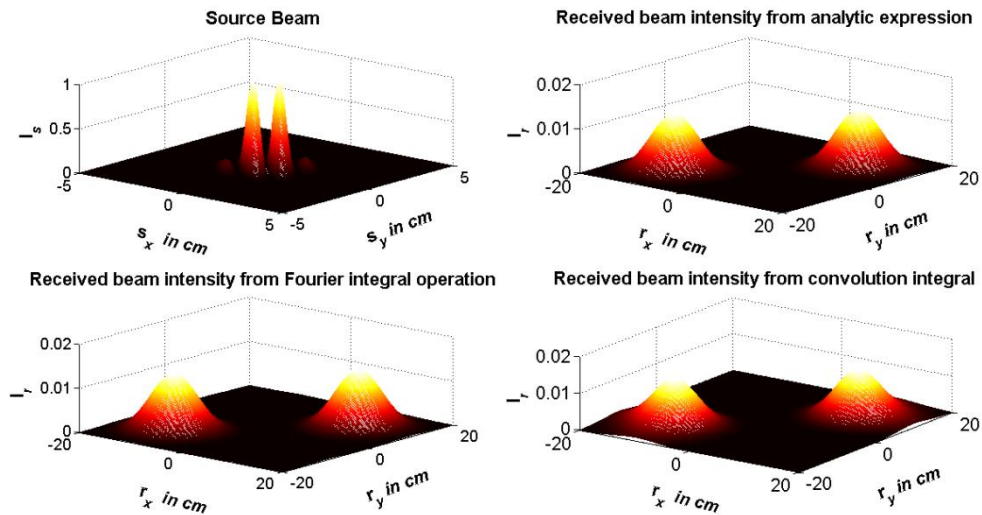

Figure 2-11 Intensity distributions of a Sine-Gaussian beam.

Total received intensity difference between analytic expression and Fourier integral operator is 0.0483 %, difference between analytic expression and convolution integral is 1.1671 %. Fig. (2-12) shows the difference between the received beam intensities which are obtained from analytic expression and Fourier integral operator.
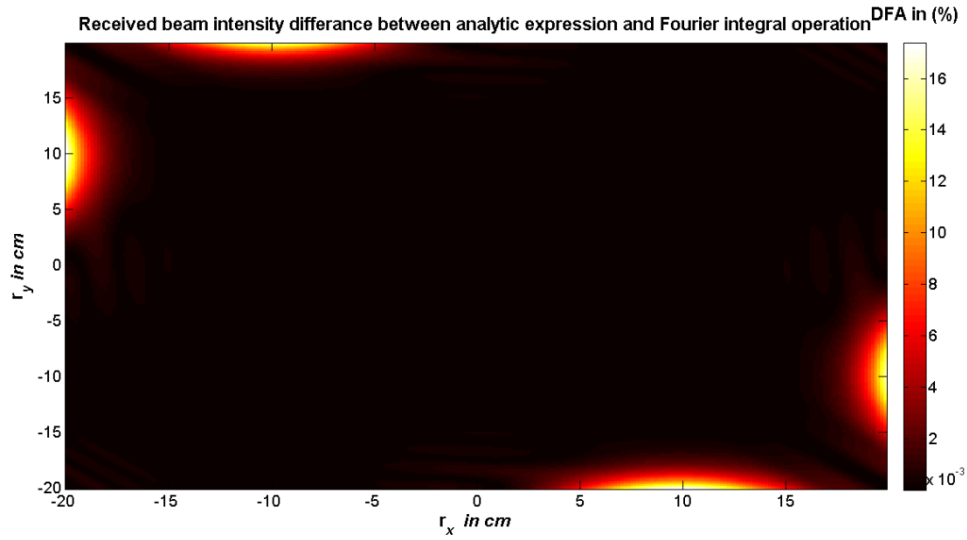
Figure 2-12 Received intensity difference of Sine-Gaussian beam between analytic expression and Fourier integral operator .

Fig. (2-13) shows the difference between the received beam intensities which are obtained from analytic expression and Fourier integral operator.
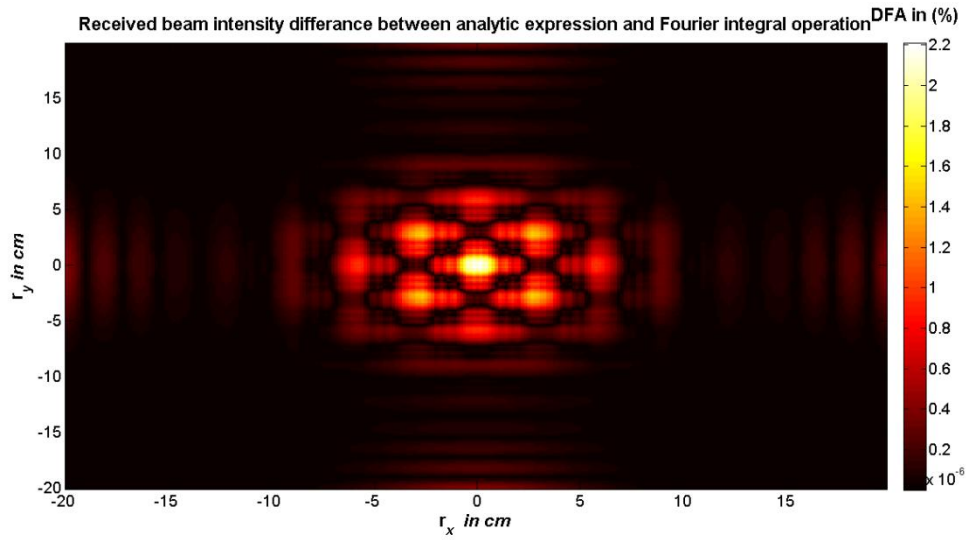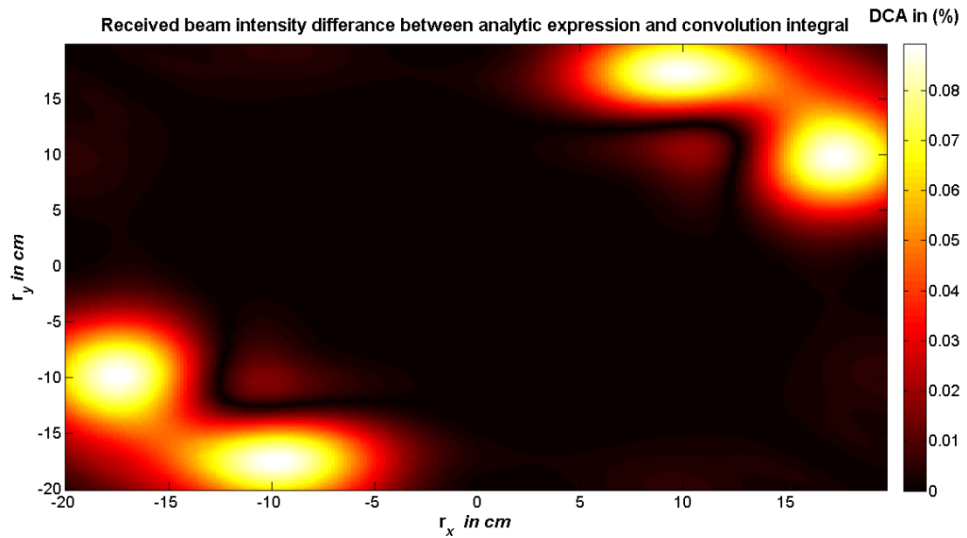

Figure 2-13 Received intensity difference of Sine-Gaussian beam between analytic expression and convolution integral.

2.7.5 Sinh-Gaussian Beam

Fig. (2-14) shows the intensity distribution of Sinh-Gaussian beam on source plane and receiver plane. Receiver plane intensity distributions obtained respectively by analytic expression, Fourier integral operator and Convolution integral. The propagation distance between source and receiver plane is L=2 km . Multiplying factor is $m_f = 4$. The Gaussian beam parameters are $\lambda = 1.55 \mu m$, $W_{s1} = W_{s2} = 1cm$, $A_{c1} = 0.5$, $A_{c2} = -0.5$, $D_{x1} = D_{y1} = -200m^{-1}$, $D_{x2} = D_{y2} = 200m^{-1}$
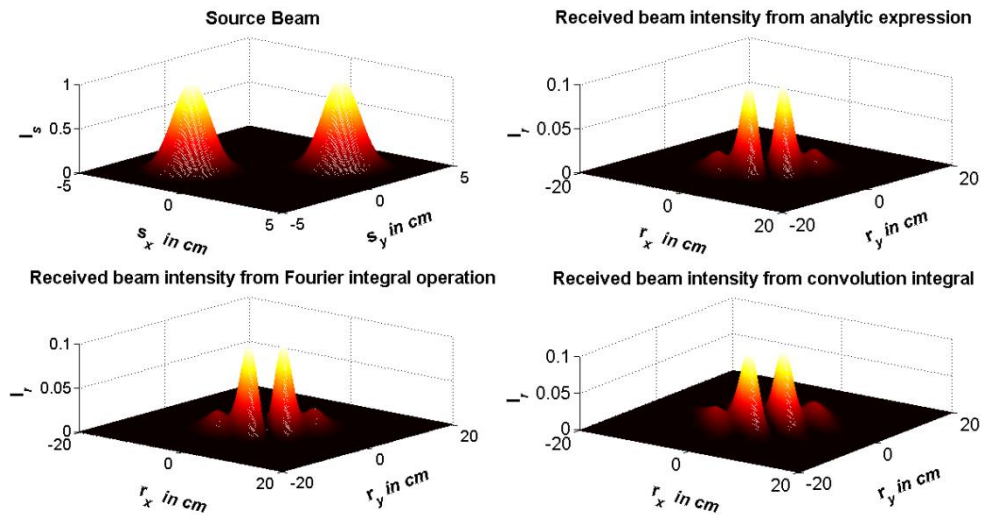
Figure 2-14 Intensity distributions of Sinh-Gaussian beam.

Total received intensity difference between analytic expression and Fourier integral operator is 0.0172 %, difference between analytic expression and convolution integral is 0.4981 %. Fig. (2-15) shows the difference between the received beam intensities which are obtained from analytic expression and Fourier integral operator.
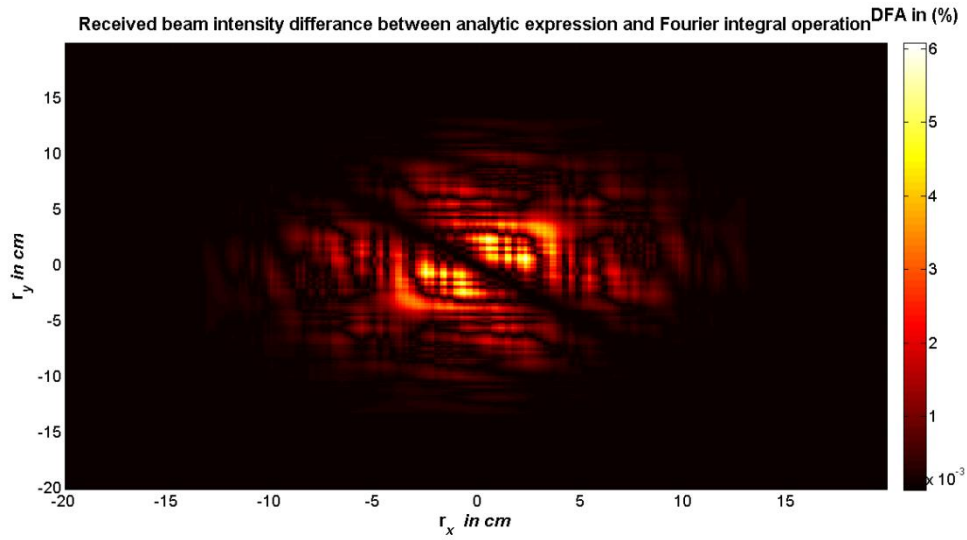
Figure 2-15 Received intensity difference of Sinh-Gaussian beam between analytic expression and Fourier integral operator .

Fig. (2-16) shows the difference between the received beam intensities which are obtained from analytic expression and Fourier integral operator.
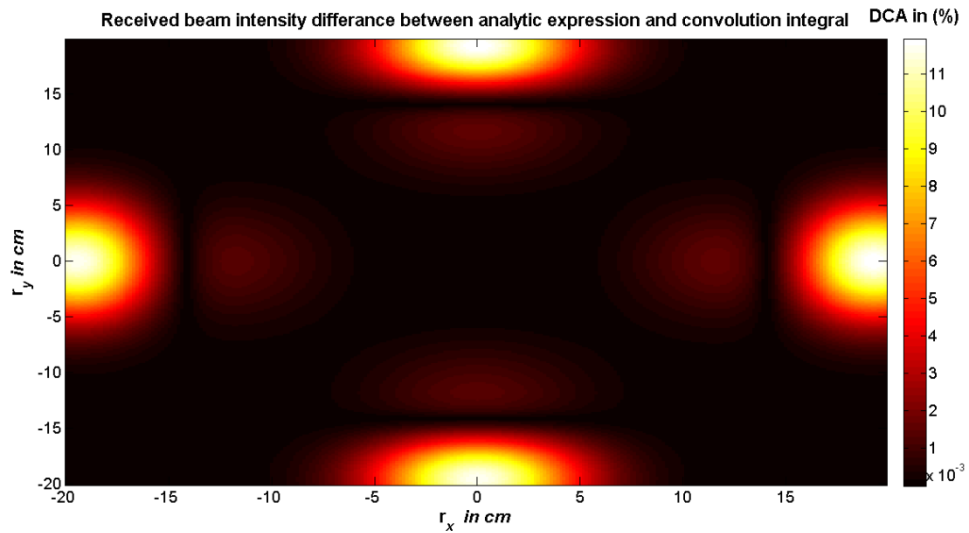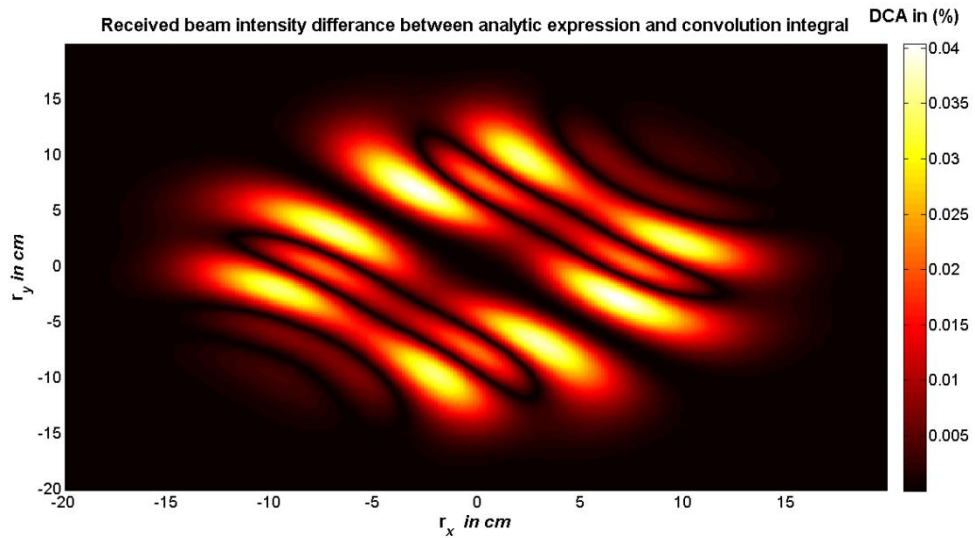

Figure 2-16 Received intensity difference of Sinh-Gaussian beam between analytic expression and convolution integral.

2.7.6 Annular Gaussian Beam

Fig. (2-17) shows the intensity distribution of Annular beam on source plane and receiver plane. Receiver plane intensity distributions obtained respectively by analytic expression, Fourier integral operator and Convolution integral. The propagation distance between source and receiver plane is L=2 km . Multiplying factor is $m_f = 4$. The beam parameters are $\lambda = 1.55\mu m$, $W_{s1} = 2cm$, $W_{s2} = 1cm$ $A_{c1} = 0.5$, $A_{c2} = -0.5$, $D_{x1} = D_{y1} = 0m^{-1}$, $D_{x2} = D_{y2} = 0m^{-1}$
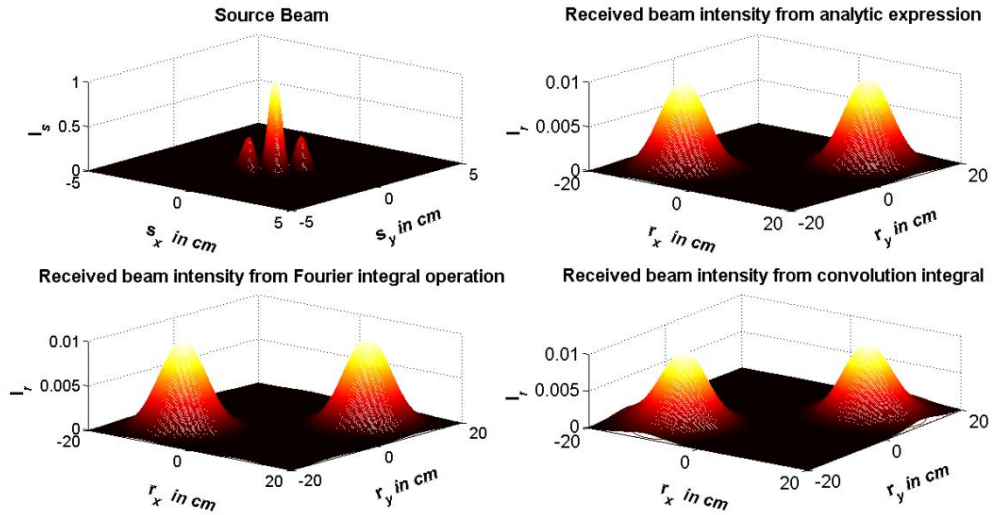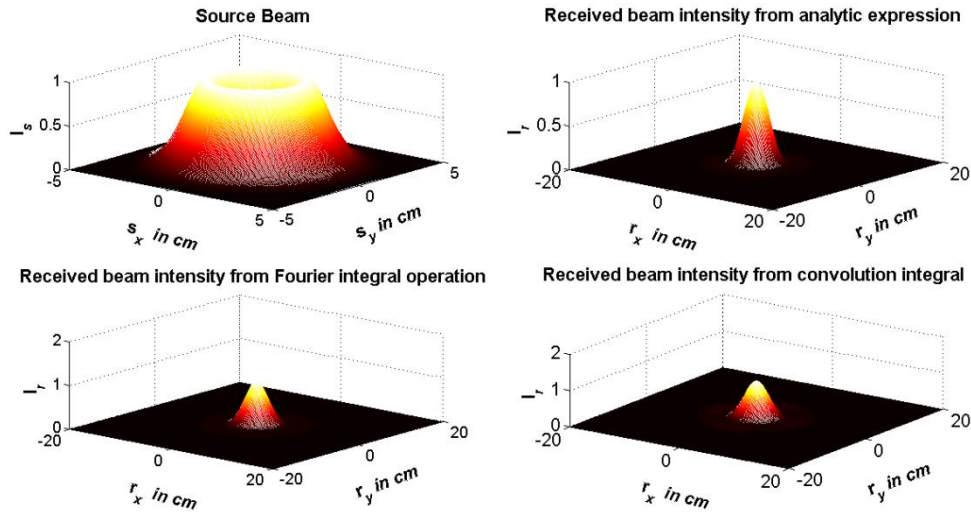

Figure 2-17 Intensity distributions of Annular Gaussian beam.

Total received intensity difference between analytic expression and Fourier integral operator is 0.0606%, difference between analytic expression and convolution integral is 0.2116%. Fig. (2-18) shows the difference between the received beam intensities which are obtained from analytic expression and Fourier integral operator.
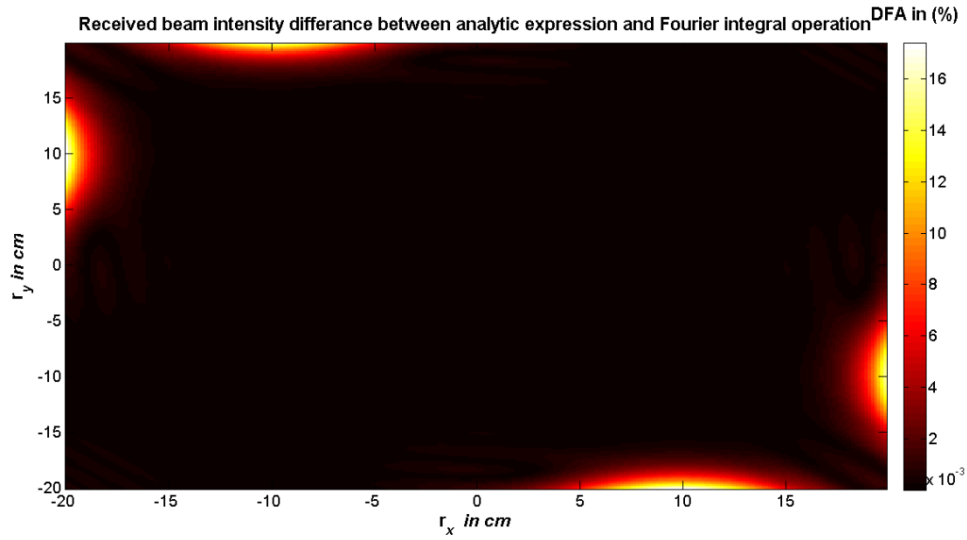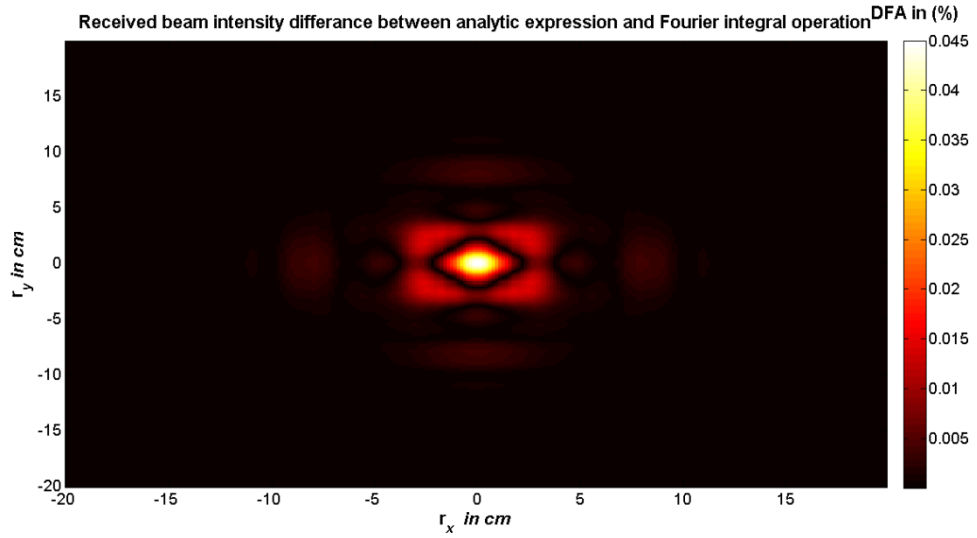
Figure 2-18 Received intensity difference of Annular Gaussian beam between analytic expression and Fourier integral operator .

Fig. (2-19) shows the difference between the received beam intensities which are obtained from analytic expression and Fourier integral operator.
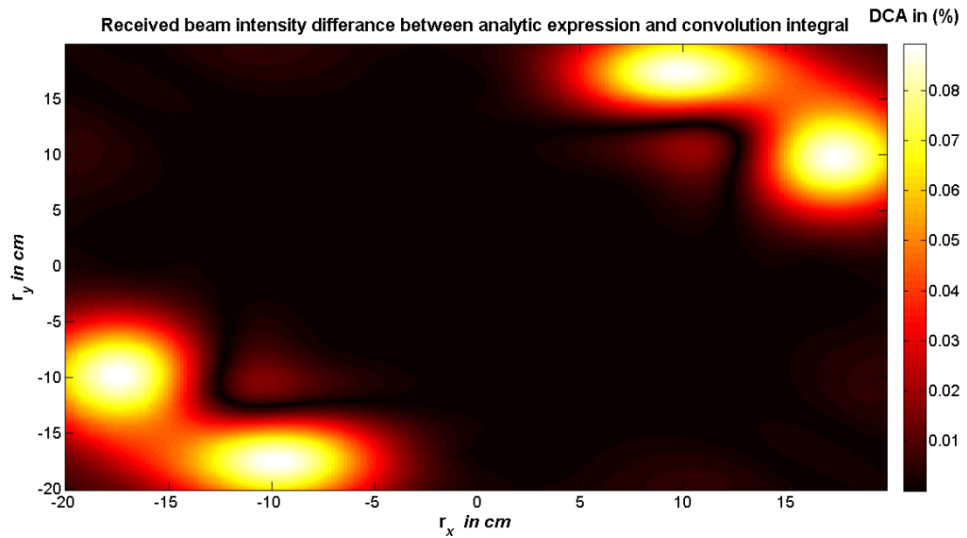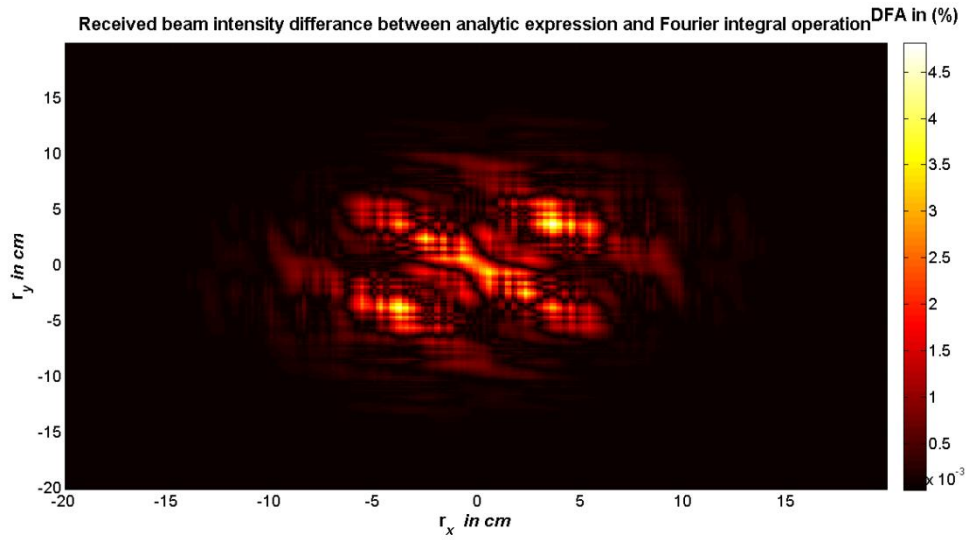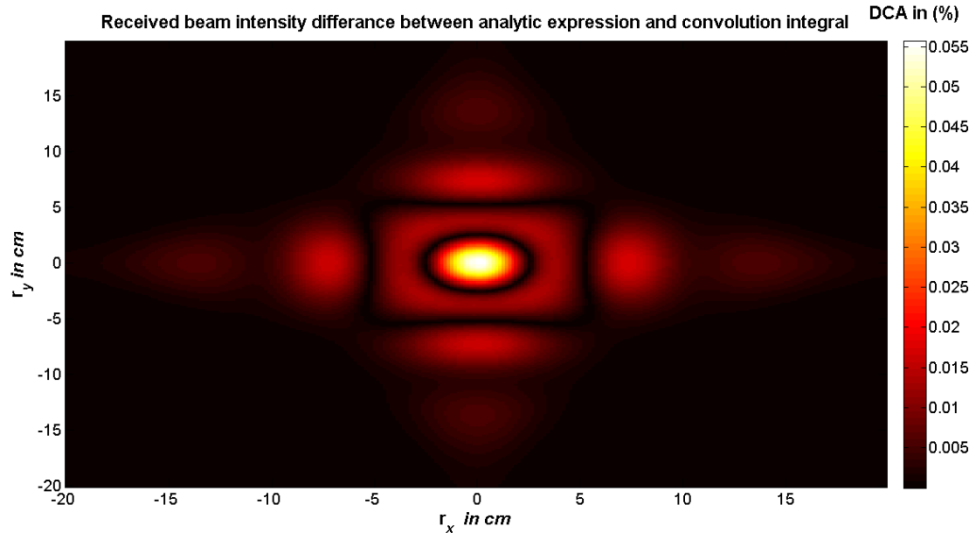

Figure 2-19 Received intensity difference of Annular Gaussian beam between analytic expression and convolution integral.

CHAPTER 3

RESULTS AND DISCUSSIONS

In this section received intensity profiles from Fourier integral operation and convolution integral are compared with the results which are obtained from analytic solution. The comparisons are made and tabulated in appendix B at different beam types and beam parameters such as wavelength (λ) in nm, amplitude coefficient (Ac) in Volt/m or Ampere/m, beam waist (w_s) in cm, different number of grids (N) and different distances (L) in km with related multiplying factor (m_f). In appendix B detailed measurements and beam parameters are available and DFA refers to difference between Fourier integral operator and analytic solution, and DCA refers to difference between convolution integral and analytic solution, both comparisons made in percentage (%) form.

3.1 Received Field Comparisons According to Wavelength

We have calculated the received beam intensities from computational models and analytic results, then we make the comparisons at different wavelengths. The wavelength range starts from the beginning of visible spectrum and ends at middle infrared wavelengths. The comparisons according to wavelengths with detailed parameters are tabulated in appendix B.1 to B.6, within the order of Gaussian beam, Cos-Gaussian beam, Cosh-Gaussian beam, Sine-Gaussian beam, Sinh-Gaussian beam and Annular Gaussian beam. In Figs (3.1) and (3.2) beam profile comparisons are shown with difference ratios.
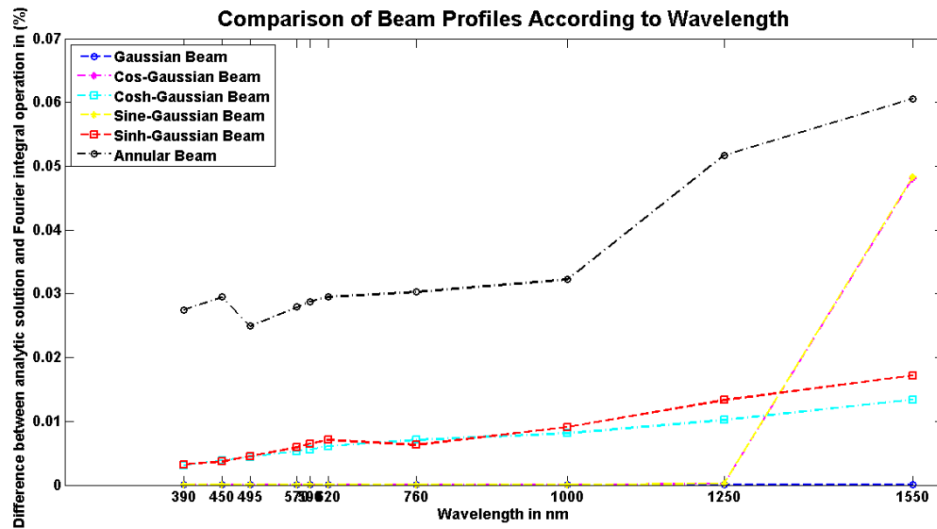
Figure 3-1 Comparison of beam profiles from analytic solution and Fourier integral operation according to wavelength

Figure (3-1) and Tables B.1 to B.6 in appendix B show that all beam profiles have increasing difference against wavelength increases. Annular beam has highest difference percentage and Gaussian beam has the lowest difference percentage for all wavelengths. Cos-Gaussian and Sine-Gaussian beams has lower difference percentage than their related hyperbolic Gaussian beams but after 1250 nm Cos-Gaussian and Sine-Gaussian beams' difference percentage became higher than hyperbolic ones. The average difference between Fourier integral operation and analytic solution is less than 1/10000 which is an acceptable ratio for Matlab's correlation tool.
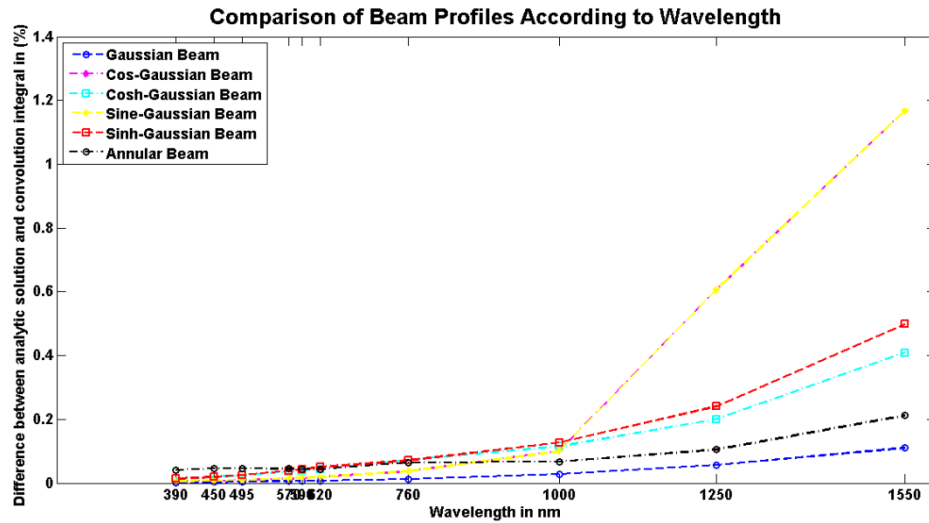
Figure 3-2 Comparison of Beam profiles from analytic solution and convolution

integral according to wavelength

Figure (3-2) and Tables B.1 to B.6 in appendix B show that all beam profiles has an increasing difference while wavelength increases. In this case Gaussian beam has the lowest difference ratio for all wavelengths but hyperbolic beams has the highest difference ratio for visible spectrum, and for infrared wavelengths Cos-Gaussian and Sine-Gaussian beams has the highest. When two computational models are compared in wavelength category convolution integral has 10 times bigger averaged ratio than Fourier integral operation.

3.2 Received Field Comparisons According to Number of Grids

Grid spacing represents step sizes in source and receiver planes. It can be predicted that bigger step size gives lower difference ratio, in analytic calculations grid spacing accepted as zero, but in discrete calculations in Matlab grid spacing should be chosen as a finite value. We have calculated the received beam intensities from computational models and analytic results, then we make the comparisons at 5 different number of

grids. The grid spacing range starts from 32 and gets double of previous one until we reach 512. The comparisons according to number of grids are shown in Tables B.7 to B.12 in appendix B, within the order of Gaussian beam, Cos-Gaussian beam, Cosh-Gaussian beam, Sine-Gaussian beam, Sinh-Gaussian beam and Annular Gaussian beam. In figs (3-3) and (3-4) beam profile comparisons are shown.
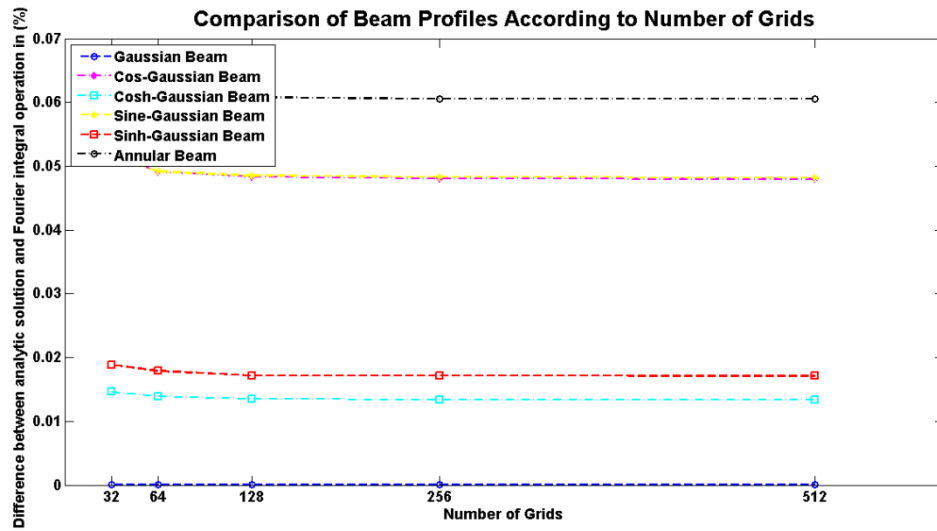
Figure 3-3 Comparison of beam profiles from analytic solution and Fourier integral operation according to grid spacing
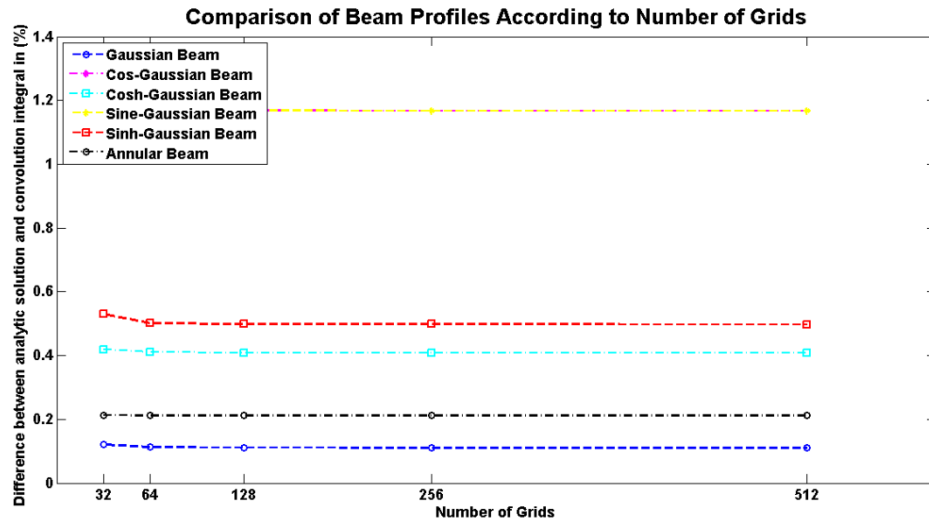
Figure 3.4 Comparison of beam profiles from analytic solution and convolution

integral according to grid spacing

In this part, since the calculations made in 1550nm wavelength, comparing the effect of grid spacing is more logical than comparing the beam profiles. Figs (3.3) and (3.4), and Tables B.7 to B.12 in appendix B shows that when the grid spacing increases the difference ratio decreases. For both computational models it shows that almost there is no difference between 256 and 512 grid points, so for computation times and effort of computer it is more convenient to choose 256 spaces.

3.3 Received Field Comparisons According to Beam Waist

In this section received beam profiles are compared with respect to beam waist. The beam waist variation starts at 0.5 cm and ends at 2 cm. For Annular Gaussian beam second beam waist is always taken half of first one.
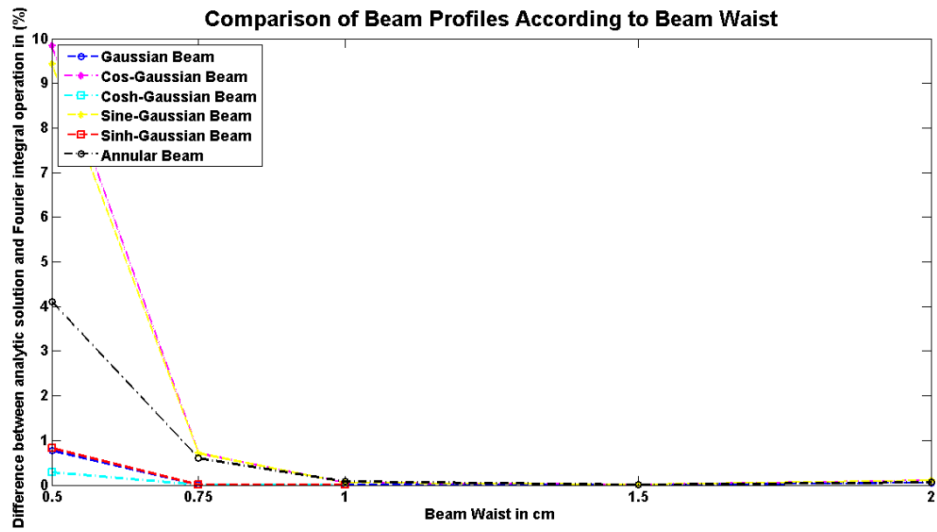
Figure 3.5 Comparison of beam profiles from analytic solution and Fourier integral operation according to beam waist
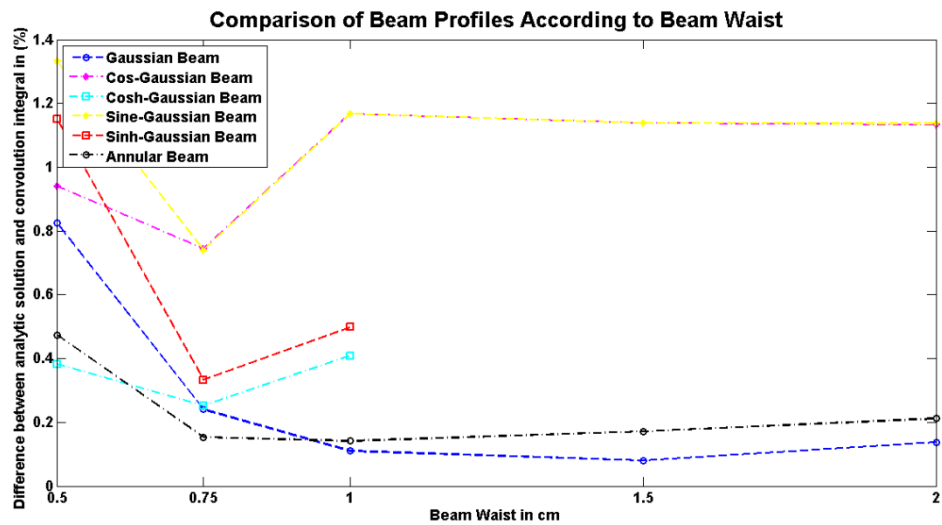
Figure 3-6 Comparison of beam profiles from analytic solution and convolution integral according to beam waist

Figs (3-5), and (3-6) and Tables B.13 to B.18 in appendix B show that Gaussian beam has very low difference ratio. Hyperbolic beams has no exact solution for the beam waists are higher than 1 cm. The reason of that hyperbolic beams become very large in

source plane, in the contrary sine and cosine Gaussian beams has a decreasing difference ratio while beam waist increases. This can be explained by the fact that while hyperbolic beams propagates they turn into their sinusoidal forms and vice versa [17]. Difference ratio of Annular Gaussian beam firstly decreases then increases. If fig (3.6) is analyzed attentively it is seen that whilst the beam waist is 0.5 cm all beam types has the lowest difference ratio except Gaussian beam.

.

Received Field Comparisons According to Propagation Distance and Related Multiplying factor

In Chapter 2 we mentioned that the relation between propagation distance (in meters), and multiplying factor (m_f), has 1/500 ratio only if the propagation ratio is more than 500 m, otherwise multiplying factor is taken as 1. In this section we computed the received intensity difference in various propagation distances with related multiplying factors, propagation distances start from 100m and extend to 100km and multiplying factor range is starts from 1 and extends to 200.
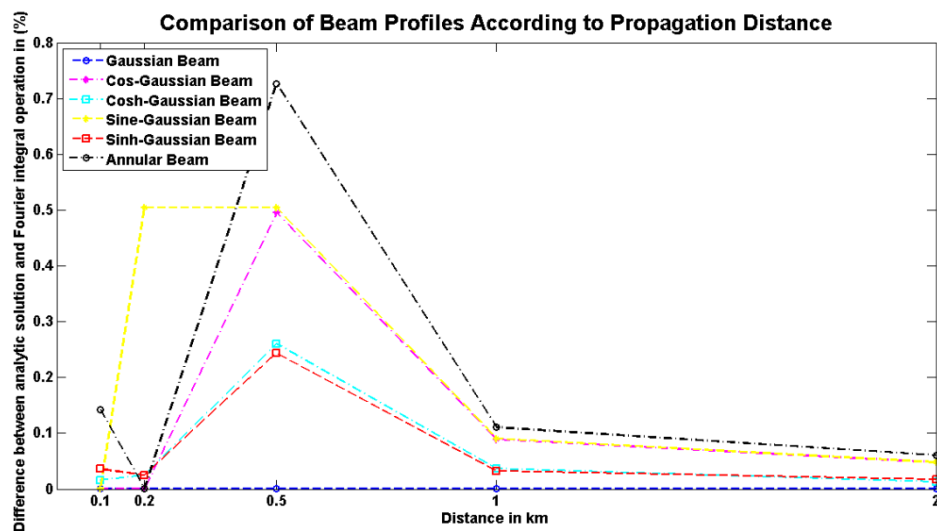
Figure 3-7 Comparison of beam profiles from analytic solution and Fourier integral operation according distances from 100 m to 2 km and related multiplying factor
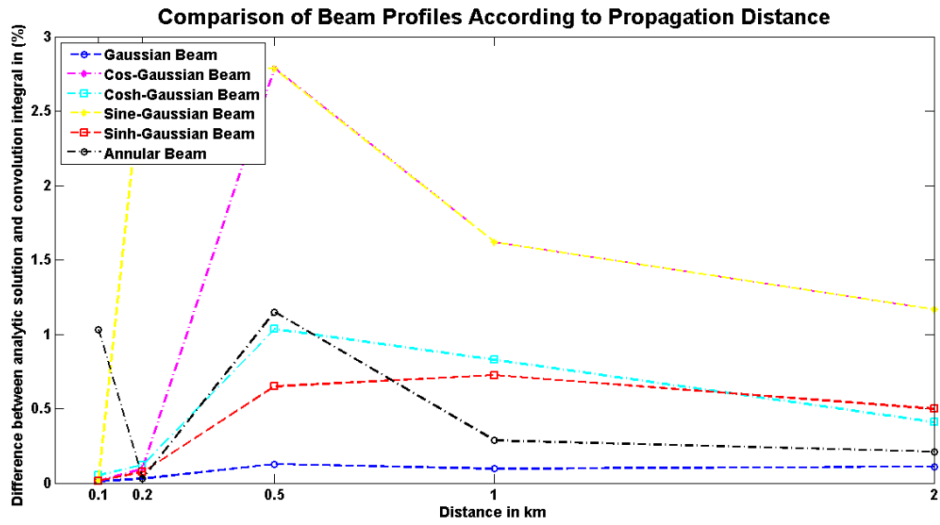
Figure 3-8 Comparison of beam profiles from analytic solution and convolution integral according distances from 100 m to 2 km and related multiplying factor
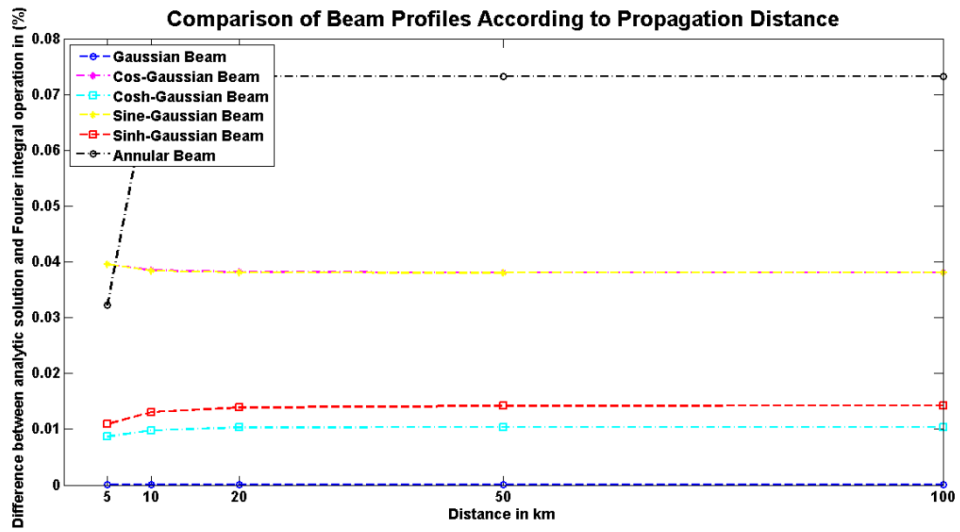
Figure 3-9 Comparison of beam profiles from analytic solution and Fourier integral operation according distances from 5 km to 100 km and related multiplying factor
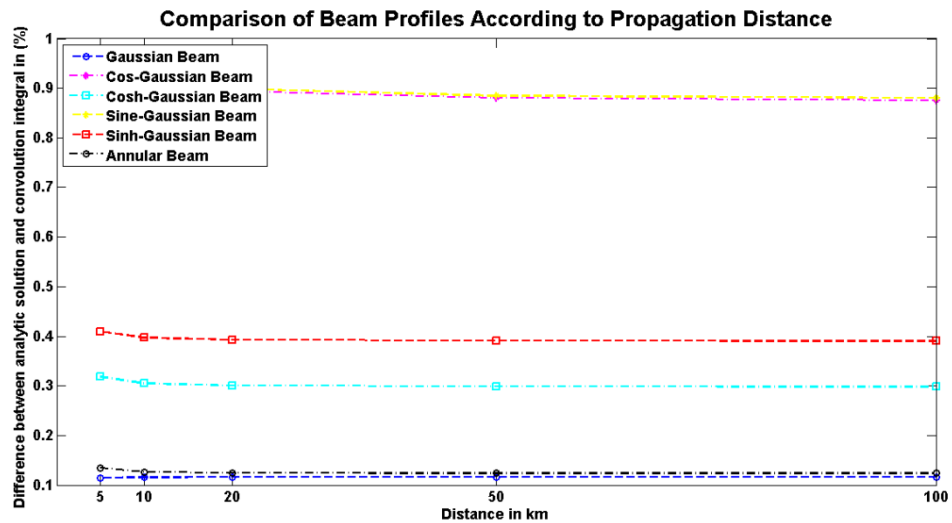
Figure 3-10 Comparison of beam profiles from analytic solution and convolution integral according distances from 5 km to 100 km and related multiplying factor

For making comparisons, distance is the most important parameter for obtaining multiplying factor. Figures (3-7) and (3-8) shows differences for distances from 100 m to 2 km and figs (3-9) and (3-10) shows differences for distances from 5 km to 100 km. From figures it is seen that for short propagation distances, the difference ratio is higher than longer distances especially for 500 m all beam types have their maximum difference ratio. For all beam types, it is observed that while the distance increases the difference ratio decreases, which is an expected result because while beams are propagation they lose the their power it means for higher propagation distances total power of beam converges to so for all solution comparing very little amount of intensities gives us very little differences. For all distances Gaussian beam difference ratio is too small that can be acceptable as zero for both computational models. Annular Gaussian beam has lower than 0.1% difference ratio for Fourier transform operation and has a little bit higher than 0.1% for convolution method. Cos-Gaussian and Sine-Gaussian beams has almost same difference ratios after 500 m, it is around 0.01% for Fourier transform operation and 1% for convolution method. The reason of that similar difference ratio is propagation characteristics of these two beams are same, on source plane they both placed on center, and while propagation, they start to move away from the center. Cosh-Gaussian and Sinh-Gaussian also have similar difference ratios since

their propagation characteristic are similar to each other and opposite to their non-hyperbolic beams, for Fourier integral operation the distances shorter than 2 km the average difference ratio is 0.1% and for longer propagation distances the ratio decreases to 0.04%, for convolution operation in short distances difference average difference ratio is around %1 for longer distances it becomes 0.35%.

CHAPTER 4

CONCLUSIONS

In this study , to make comparisons we have taken computational model solution of Huygens-Fresnel integral and compared it to its analytic solution. These comparisons show that Fourier integral operation has lower difference ratio than convolution theorem, the reason of that difference is convolution theorem solution gives over-propagated form of beam it can be seen exactly in figs (2-11) and (2-13). For analytic solution we assumed source plane and receiver are infinite but for computational modes we have limited source plane in other words the output of resonator as 10cm, and it behaved like a rectangular aperture. This aperture added a sinc function diffraction effect in propagation simulations, but for Fourier integral operation it is very small that can be neglected, in contrary for convolution theorem the diffraction effect of this aperture is more obvious.

REFERENCES

[1]   Voelz, D. (2011). Computational Fourier Optics. Washington: SPIE Press.

[2]   J. Jahns, S. Helfert*. (2012). Introduction to Micro and Nano optics. Wienheim:Wiley-VCH

[3]   SALEH, B. E. A., TEICH, M.C. (1991), Fundamentals of Photonics. New Jersey:John Wiley&Sons Inc.

[4]   Electromagnetic Spectrum, retrieved from: http://www.globalspec.com/ImageRepository/LearnMore/20131/Visible%20 spectrumb4a51119b4694d90a49ee0c0004a4da0.png, on 21 December 2012

[5]   Tan,S.M. Linear Systems. The University of Auckland 453.701, retrieved from http://home.comcast.net/~szemengtan/LinearSystems/waves.pdf, on 27 February 2013.

[6]   GRADSHTEYN, I.S., RYZHIK, I.M. (2000), Tables of Integrals, Series and Products, Academic Press, New York.

[7]   Siegman, A.E. (1986). Lasers. Sausaluto: The Mapple-Vali Book Manufacturing Group

[8]   ANDREWS, L. C. (2004), Field Guide to Atmospheric Optics. Bellingham, Washington: SPIE Press.

[9]   KOGELNIK, H., LI, H. (1966), Laser Beams and Resonators, Applied Optics, 1550- 1567. Vol. 5.

[10]   Schmidt, J.D. (2010) Numerical Simulation of Optical Wave Propagation in Matlab: Washington: SPIE press.

[11]   Tyler, G.A, and Fried, D.L. (1982). A wave optics propagation algorithm. Optical Sciences Company, TR-451.

[12]   Kamacıoğlu C. and Baykal Y. (2012) ,Generalized expression for optical source fields. Opt. Lasers Technol., 44 (6), 1706-1712.

[13]   Eyyuboğlu H.T. Notes for ECE 635. Çankaya University, retrieved from, http://ece646.cankaya.edu.tr/uploads/files/Notes%20for%20ECE%20635_Eylul%202011.pdf, on 26 July 2012.

[14]   ARPAL(, Ç. et. al. (2006), Simulator for General-Type Beam Propagation in Turbulent Atmosphere, Opt. Express, 8918-8928. Vol. 14.

[15]   Eyyuboğlu, H. T. (2007). Hermite hyperbolic / sinusoidal Gaussian beams in ABCD systems. Optik 118(6), 289-295

[16]   Eyyuboğlu, H. T. (2013). Estimation of aperture averaged scintillations in weak turbulence regime for annular, sinusoidal and hyperbolic Gaussian beams using random phase screen, Optics & Laser Technology, vol. 52, 96-102

[17]   Eyyuboğlu, H. T. (2007). Hermite hyperbolic / sinusoidal Gaussian beams in ABCD systems. Optik 118(6), 289-295

APPENDIX A

MATLAB CODE

```matlab
% This program compares the free space intensities of hyp / sino beams
% from analytic derivation, FT and angular spectrum methods
function computeandcompare
clear;clc;clf;warning off all;close all;format short
Lmax = 2;

%%% Source beam parameters
ALarr = [1 0;0.5 0.5;0.5 0.5;0.5*j -0.5*j;0.5 -0.5;0.5 -0.5];  % Amplitude Matrix
Dmat = [0 25 50 100 200 400];% Displacement parameter matrix

%Beam waist matrices
alfasxarr = [1e-2 1e-2;1e-2 1e-2;1e-2 1e-2;1e-2 1e-2;1e-2 1e-2;2e-2 1e-2];
alfasxarr = alfasxarr*1.0;

alfasyarr = [1e-2 1e-2;1e-2 1e-2;1e-2 1e-2;1e-2 1e-2;1e-2 1e-2;2e-2 1e-2];
alfasyarr = alfasyarr*1.0;

ibmax = 1; %%% Choosing beam type 1 for Gaussian, 2 for Cos-Gaussian,
%3 for Cosh-Gaussian, 4 for Sine-Gaussian, 5 for Sinh-Gaussian, 6 for Annular
beam

N = 256; %Number of grids
SL=10e-2; %Source Length
```

```matlab
d1 = SL/N;
L = 2e3; %Propagation distance
lamda = 1550e-9; %Wavelength
k = 2*pi/lamda;
mf =4; %Multiplying factor
d2 = mf*d1;


Dsarr = [j*Dmat(1) -j*Dmat(1);-j*Dmat(5) j*Dmat(5);
         Dmat(5) -Dmat(5);-j*Dmat(5) j*Dmat(5);
         -Dmat(5) Dmat(5) ;1*Dmat(1) -1*Dmat(1)];
Fsarr = [5e15 5e15;5e15 5e15;5e15 5e15;5e15 5e15;5e15 5e15;5e15 5e15];
alfaxarr = 1./(k*alfasxarr.^2) + j./(2*Fsarr);
alfayarr = 1./(k*alfasyarr.^2) + j./(2*Fsarr);


[nx ny ] = meshgrid(-N/2 : N/2-1);
sx = nx*d1;
sy = ny*d1;
rx = nx*d2;
ry = ny*d2;


s=-SL/2:d1:SL/2-d1;
r=mf*s;


%Generating Beams
for ib = ibmax
    uran = zeros(N, N);
    for LL = 1:Lmax
    alfax = alfaxarr(ib,LL);
    alfay = alfayarr(ib,LL);
    Dx = Dsarr(ib,LL)
    Dy = Dsarr(ib,LL)
    AL = ALarr(ib,LL)
```

```matlab
  us1 = AL*exp(-0.5*k*sx.^2*alfax - 0.5*k*sy.^2*alfay + Dx*sx + Dy*sy);
us = us + us1;
uran1 = AL/sqrt(1 + j*alfax*L)/sqrt(1 + j*alfay*L)*exp(-0.5*k*alfax*rx.^2/(1 +
j*alfax*L)).* ....
   exp(rx*Dx/(1 + j*alfax*L)).*exp(j*0.5*Dx^2*L/k/(1 + j*alfax*L)).* ....
   exp(-0.5*k*alfay*ry.^2/(1 + j*alfay*L)).*exp(ry*Dy/(1 +
j*alfay*L)).*exp(j*0.5*Dy^2*L/k/(1 + j*alfay*L));
uran = uran1 + uran;end;end
Is = us.*conj(us);
Iran = uran.*conj(uran);
 %%%%% Fourier Transform Method
df1 = 1/(N*d1);[fx fy] = meshgrid((-N/2 : N/2-1) * df1);
urft = exp(j*k/2*(mf - 1)/(mf*L)*(rx.^2 + ry.^2)).*ift2(exp(-j*pi^2*2*L/mf/k*(fx.^2
+ fy.^2)).*ft2(us.*exp(j*k*(1 - mf)/(2*L)*(sx.^2 + sy.^2))/mf,d1),df1);
Irft = urft.*conj(urft);
 %%%%% Convolution  Method
hsxsy = exp(j*k/(2*L)*mf*(sx.^2 + sy.^2));
us1 = us.*exp(j*k*(1- mf)*(sx.^2 + sy.^2)/(2*L));
urcm = -j*k/(2*pi*L)*exp(j*k*L)*exp(j*k*(mf - 1)*(rx.^2 +
ry.^2)/(2*L*mf)).*conv2(us1,hsxsy,'same')*d1^2;
Ircm = urcm.*conj(urcm);


if ibmax==3||5    %to normalize the hyperbolic beams
   Iran=Iran/max(max(Is));
   Irft =Irft/max(max(Is));
   Ircm = Ircm/max(max(Is));
   Is=Is/max(max(Is));
else
   Is=Is;
   Iran=Iran;
   Irft=Irft;
   Ircm=Ircm;
```

```matlab
end

figure(1)%3d plots
subplot(2,2,1)
meshc(sx/1e-2,sy/1e-2,Is);view([40 35]);colormap([0 0 0]);
title('Source Beam ', 'Fontsize',16');set(gcf,'Color',[1 1 1]);set(gca,'FontSize',14)
xlabel('Sx  in cm','FontSize',10,'FontWeight','bold','Rotation',-14);
ylabel('Sy in cm','FontSize',10,'FontWeight','bold','Rotation',25)
zlabel('Is ','FontSize',12,'FontWeight','bold')

subplot(2,2,2)
meshc(rx/1e-2,ry/1e-2,Iran);view([40 35]);colormap([0 0 0]);
title('Received beam intensity from analytic expression ',
'Fontsize',16');set(gcf,'Color',[1 1 1]);set(gca,'FontSize',14)
xlabel('Rx  in cm','FontSize',10,'FontWeight','bold','Rotation',-15);
ylabel('Ry in cm','FontSize',10,'FontWeight','bold','Rotation',25)
zlabel('Ir ','FontSize',12,'FontWeight','bold')

subplot(2,2,3)
meshc(rx/1e-2,ry/1e-2,Irft);view([40 35]);colormap([0 0 0]);
title('Received beam intensity from Fourier integral operator ',
'Fontsize',16');set(gcf,'Color',[1 1 1]);set(gca,'FontSize',14)
xlabel('Rx  in cm','FontSize',10,'FontWeight','bold','Rotation',-15);
ylabel('Ry in cm','FontSize',10,'FontWeight','bold','Rotation',25)
zlabel('Ir ','FontSize',12,'FontWeight','bold')

subplot(2,2,4)
meshc(rx/1e-2,ry/1e-2,Ircm);view([40 35]);colormap([0 0 0]);
title('Received beam intensity from convolution integral ',
'Fontsize',16');set(gcf,'Color',[1 1 1]);set(gca,'FontSize',14)
xlabel('Rx  in cm','FontSize',10,'FontWeight','bold','Rotation',-15);
ylabel('Ry in cm','FontSize',10,'FontWeight','bold','Rotation',25)
```

```matlab
zlabel('Ir ','FontSize',12,'FontWeight','bold')


% %%%%%%2D Plots%%%%
% figure(2)
% subplot(2,2,1)
% imagesc(s/1e-2,s/1e-2,Is);
% title('Source Beam ', 'Fontsize',16');colormap('gray');set(gca,'FontSize',14)
% xlabel('Sx  in cm','FontSize',10,'FontWeight','bold');
% ylabel('Sy in cm','FontSize',10,'FontWeight','bold')
%
% subplot(2,2,2)
% imagesc(r/1e-2,r/1e-2,Iran);
% title('Received beam intensity from analytic expression ',
'Fontsize',16');set(gcf,'Color',[1 1 1]);set(gca,'FontSize',14)
% xlabel('Rx  in cm','FontSize',10,'FontWeight','bold');
% ylabel('Ry in cm','FontSize',10,'FontWeight','bold');
%

% subplot(2,2,3)
% imagesc(r/1e-2,r/1e-2,Irft);
% title('Received beam intensity from Fourier integral operator ',
'Fontsize',16');set(gcf,'Color',[1 1 1]);set(gca,'FontSize',14)
% xlabel('Rx  in cm','FontSize',10,'FontWeight','bold');
% ylabel('Ry in cm','FontSize',10,'FontWeight','bold') ;
%
% subplot(2,2,4)
% imagesc(r/1e-2,r/1e-2,Ircm);
% title('Received beam intensity from convolution integral ',
'Fontsize',16');set(gcf,'Color',[1 1 1]);set(gca,'FontSize',14)
% xlabel('Rx  in cm','FontSize',10,'FontWeight','bold');
% ylabel('Ry in cm','FontSize',10,'FontWeight','bold');
```

```matlab
% Making Comparison
Irand=Iran./max(max(Iran));
Ircmd=Ircm./max(max(Iran));
Idiff = zeros(N, N);
for l=1:N
   for k=1:N
      Idiff(l,k)=abs(Irand(l,k)-Ircmd(l,k));
   end;end;

Idiffav=0;
for l=1:N
   for k=1:N
      Idiffav=Idiffav+Idiff(l,k);
   end;end;
Idiffav=100*Idiffav/N^2;
Idiffcm=Idiffav

% Plotting difference matrix

figure(3)
imagesc(r/1e-2,r/1e-2,Idiff);
title('Received beam intensity differance between analytic expression and
convolution integral ', 'Fontsize',16');set(gca,'FontSize',14);
colormap('gray');
xlabel('Rx  in cm','FontSize',10,'FontWeight','bold');
ylabel('Ry in cm','FontSize',10,'FontWeight','bold') ;
axis xy;

Irftd=Irft./max(max(Iran));
Idiff2 = zeros(N, N);
```

```matlab
for m=1:N
    for n=1:N
        Idiff2(m,n)=abs(Irand(m,n)-Irftd(m,n));
    end;end;
Idiff2av=0;
for l=1:N
    for k=1:N
        Idiff2av=Idiff2av+Idiff2(l,k);
    end;end;
Idiff2av=100*Idiff2av/N^2;
Idifffft=Idiff2av

% Plotting difference matrix

figure(4)
imagesc(r/1e-2,r/1e-2,Idiff2);
title('Received beam intensity differance between analytic expression and Fourier
integral operator ', 'Fontsize',16');set(gca,'FontSize',14);
colormap('gray');
xlabel('Rx  in cm','FontSize',10,'FontWeight','bold');
ylabel('Ry in cm','FontSize',10,'FontWeight','bold') ;
axis xy;

%%%% fft and ifft functions used
function G = ft2(g, delta)
G = fftshift(fft2(fftshift(g))) * delta^2;
function g = ift2(G, delta_f)
    N = size(G, 1);
    g = ifftshift(ifft2(ifftshift(G))) * (N * delta_f)^2;
```

APPENDIX B

DETAILED RECEIVED INTENSITY DIFFERANCE TABLES

3.1 Received Field Tables According to Wavelength

Table B.1 Gaussian beam received intensity differences according to wavelength

A_{c1}	A_{c2}	W_{s1}	W_{s2}	D_1	D_2	λ	L	m_f	N	DFA x10^{-7}	DCA
1	0	1	1	0	0	**390**	2	4	256	3.2887	0.0025
1	0	1	1	0	0	**450**	2	4	256	6.6043	0.0034
1	0	1	1	0	0	**495**	2	4	256	3.7210	0.0043
1	0	1	1	0	0	**570**	2	4	256	7.6234	0.0061
1	0	1	1	0	0	**590**	2	4	256	9.6302	0.0066
1	0	1	1	0	0	**620**	2	4	256	12.148	0.0075
1	0	1	1	0	0	**760**	2	4	256	9.8670	0.0130
1	0	1	1	0	0	**1000**	2	4	256	26.454	0.0284
1	0	1	1	0	0	**1250**	2	4	256	56.948	0.0562
1	0	1	1	0	0	**1550**	2	4	256	85.502	0.1105

Table B.2 Cos-Gaussian beam received intensity differences according to wavelength

A_{c1}	A_{c2}	W_{s1}	W_{s2}	D_1	D_2	λ	L	m_f	N	DFA x10^{-6}	DCA
0.5	-0.5	1	1	200j	-200j	390	2	4	256	0.6837	0.0053
0.5	-0.5	1	1	200j	-200j	450	2	4	256	1.4293	0.0075
0.5	-0.5	1	1	200j	-200j	495	2	4	256	1.0716	0.0096
0.5	-0.5	1	1	200j	-200j	570	2	4	256	1.4790	0.0143
0.5	-0.5	1	1	200j	-200j	590	2	4	256	1.8137	0.0158
0.5	-0.5	1	1	200j	-200j	620	2	4	256	2.3755	0.0184
0.5	-0.5	1	1	200j	-200j	760	2	4	256	2.7400	0.0375
0.5	-0.5	1	1	200j	-200j	1000	2	4	256	4.8096	0.1004
0.5	-0.5	1	1	200j	-200j	1250	2	4	256	255.32	0.6056
0.5	-0.5	1	1	200j	-200j	1550	2	4	256	48083	1.1669

Table B.3 Cosh-Gaussian beam received intensity differences according to wavelength

A_{c1}	A_{c2}	W_{s1}	W_{s2}	D_1	D_2	λ	L	m_f	N	DFA	DCA
0.5	0.5	1	1	200	-200	390	2	4	256	0.0031	0.0137
0.5	0.5	1	1	200	-200	450	2	4	256	0.0039	0.0192
0.5	0.5	1	1	200	-200	495	2	4	256	0.0044	0.0245
0.5	0.5	1	1	200	-200	570	2	4	256	0.0053	0.0354
0.5	0.5	1	1	200	-200	590	2	4	256	0.0056	0.0387
0.5	0.5	1	1	200	-200	620	2	4	256	0.0061	0.0440
0.5	0.5	1	1	200	-200	760	2	4	256	0.0071	0.0729
0.5	0.5	1	1	200	-200	1000	2	4	256	0.0081	0.1157
0.5	0.5	1	1	200	-200	1250	2	4	256	0.0102	0.2000
0.5	0.5	1	1	200	-200	1550	2	4	256	0.0134	0.4084

Table B.4 Sine-Gaussian beam received intensity differences according to wavelength

A_{c1}	A_{c2}	W_{s1}	W_{s2}	D_1	D_2	λ	L	m_f	N	DFA x10^{-6}	DCA
0.5j	-0.5j	1	1	200j	-200j	**390**	2	4	256	0.6721	0.0053
0.5j	-0.5j	1	1	200j	-200j	**450**	2	4	256	1.4403	0.0075
0.5j	-0.5j	1	1	200j	-200j	**495**	2	4	256	1.0612	0.0096
0.5j	-0.5j	1	1	200j	-200j	**570**	2	4	256	1.4640	0.0143
0.5j	-0.5j	1	1	200j	-200j	**590**	2	4	256	1.8068	0.0158
0.5j	-0.5j	1	1	200j	-200j	**620**	2	4	256	2.3805	0.0184
0.5j	-0.5j	1	1	200j	-200j	**760**	2	4	256	2.7450	0.0375
0.5j	-0.5j	1	1	200j	-200j	**1000**	2	4	256	4.7374	0.1000
0.5j	-0.5j	1	1	200j	-200j	**1250**	2	4	256	257.16	0.6057
0.5j	-0.5j	1	1	200j	-200j	**1550**	2	4	256	48294	1.1671

Table B.5 Sinh-Gaussian beam received intensity differences according to wavelength

A_{c1}	A_{c2}	W_{s1}	W_{s2}	D_1	D_2	λ	L	m_f	N	DFA	DCA
0.5	-0.5	1	1	-200	200	**390**	2	4	256	0.0032	0.0136
0.5	-0.5	1	1	-200	200	**450**	2	4	256	0.0037	0.0190
0.5	-0.5	1	1	-200	200	**495**	2	4	256	0.0045	0.0249
0.5	-0.5	1	1	-200	200	**570**	2	4	256	0.0059	0.0385
0.5	-0.5	1	1	-200	200	**590**	2	4	256	0.0065	0.0427
0.5	-0.5	1	1	-200	200	**620**	2	4	256	0.0071	0.0496
0.5	-0.5	1	1	-200	200	**760**	2	4	256	0.0063	0.0707
0.5	-0.5	1	1	-200	200	**1000**	2	4	256	0.0091	0.1266
0.5	-0.5	1	1	-200	200	**1250**	2	4	256	0.0133	0.2405
0.5	-0.5	1	1	-200	200	**1550**	2	4	256	0.0172	0.4981

Table B.6 Annular Gaussian beam received intensity differences according to wavelength

A_{c1}	A_{c2}	W_{s1}	W_{s2}	D_1	D_2	λ	L	m_f	N	DFA	DCA
0.5	-0.5	2	1	0	0	**390**	2	4	256	0.0275	0.0412
0.5	-0.5	2	1	0	0	**450**	2	4	256	0.0295	0.0465
0.5	-0.5	2	1	0	0	**495**	2	4	256	0.0249	0.0459
0.5	-0.5	2	1	0	0	**570**	2	4	256	0.0279	0.0444
0.5	-0.5	2	1	0	0	**590**	2	4	256	0.0288	0.0431
0.5	-0.5	2	1	0	0	**620**	2	4	256	0.0295	0.0442
0.5	-0.5	2	1	0	0	**760**	2	4	256	0.0303	0.0648
0.5	-0.5	2	1	0	0	**1000**	2	4	256	0.0322	0.0669
0.5	-0.5	2	1	0	0	**1250**	2	4	256	0.0517	0.1046
0.5	-0.5	2	1	0	0	**1550**	2	4	256	0.0606	0.2116

3.2 Received Field Tables According to Number of grids

Table 3.7 Gaussian beam received intensity differences according to number of grids

A_{c1}	A_{c2}	W_{s1}	W_{s2}	D_1	D_2	λ	L	m_f	N	DFA	DCA
1	0	1	1	0	0	1550	2	4	**32**	1.1986×10^{-5}	0.1212
1	0	1	1	0	0	1550	2	4	**64**	0.9600×10^{-5}	0.1130
1	0	1	1	0	0	1550	2	4	**128**	0.8742×10^{-5}	0.1110
1	0	1	1	0	0	1550	2	4	**256**	0.8550×10^{-5}	0.1105
1	0	1	1	0	0	1550	2	4	**512**	0.8494×10^{-5}	0.1103

Table B.8 Cos-Gaussian beam received intensity differences according to number of grids

A_{c1}	A_{c2}	W_{s1}	W_{s2}	D_1	D_2	λ	L	m_f	N	DFA	DCA
0.5	-0.5	1	1	200j	-200j	1550	2	4	**32**	0.0519	1.1770
0.5	-0.5	1	1	200j	-200j	1550	2	4	**64**	0.0491	1.1700
0.5	-0.5	1	1	200j	-200j	1550	2	4	**128**	0.0483	1.1687
0.5	-0.5	1	1	200j	-200j	1550	2	4	**256**	0.0481	1.1669
0.5	-0.5	1	1	200j	-200j	1550	2	4	**512**	0.0480	1.1669

Table B.9 Cosh-Gaussian beam received intensity differences according to number of grids

A_{c1}	A_{c2}	W_{s1}	W_{s2}	D_1	D_2	λ	L	m_f	N	DFA	DCA
0.5	0.5	1	1	200	-200	1550	2	4	**32**	0.0146	0.4197
0.5	0.5	1	1	200	-200	1550	2	4	**64**	0.0139	0.4110
0.5	0.5	1	1	200	-200	1550	2	4	**128**	0.0135	0.4089
0.5	0.5	1	1	200	-200	1550	2	4	**256**	0.0134	0.4084
0.5	0.5	1	1	200	-200	1550	2	4	**512**	0.0134	0.4083

Table B.10 Sine-Gaussian beam received intensity differences according to number of grids

A_{c1}	A_{c2}	W_{s1}	W_{s2}	D_1	D_2	λ	L	m_f	N	DFA	DCA
0.5j	-0.5j	1	1	200j	-200j	1550	2	4	**32**	0.0519	1.1784
0.5j	-0.5j	1	1	200j	-200j	1550	2	4	**64**	0.0492	1.1704
0.5j	-0.5j	1	1	200j	-200j	1550	2	4	**128**	0.0485	1.1689
0.5j	-0.5j	1	1	200j	-200j	1550	2	4	**256**	0.0483	1.1671
0.5j	-0.5j	1	1	200j	-200j	1550	2	4	**512**	0.0482	1.1669

Table B.11 Sinh-Gaussian beam received intensity differences according to number of grids

A_{c1}	A_{c2}	W_{s1}	W_{s2}	D_1	D_2	λ	L	m_f	N	DFA	DCA
0.5	-0.5	1	1	-200	200	1550	2	4	**32**	0.0189	0.5303
0.5	-0.5	1	1	-200	200	1550	2	4	**64**	0.0179	0.5018
0.5	-0.5	1	1	-200	200	1550	2	4	**128**	0.0172	0.4988
0.5	-0.5	1	1	-200	200	1550	2	4	**256**	0.0172	0.4981
0.5	-0.5	1	1	-200	200	1550	2	4	**512**	0.0171	0.4976

Table B.12Annular Gaussian beam Received intensity differences according to number of grids

A_{c1}	A_{c2}	W_{s1}	W_{s2}	D_1	D_2	λ	L	m_f	N	DFA	DCA
0.5	-0.5	2	1	0	0	1550	2	4	**32**	0.0667	0.2136
0.5	-0.5	2	1	0	0	1550	2	4	**64**	0.0617	0.2123
0.5	-0.5	2	1	0	0	1550	2	4	**128**	0.0608	0.2117
0.5	-0.5	2	1	0	0	1550	2	4	**256**	0.0606	0.2116
0.5	-0.5	2	1	0	0	1550	2	4	**512**	0.0606	0.2115

3.3 Received Field Tables According to Beam Waist

Table B.13 Gaussian beam received intensity differences according to beam waist

A_{c1}	A_{c2}	W_{s1}	W_{s2}	D_1	D_2	λ	L	m_f	N	DFA	DCA
1	0	**0.5**	**0.5**	0	0	1550	2	4	256	0.7716	0.8261
1	0	**0.75**	**0.75**	0	0	1550	2	4	256	0.0025	0.2407
1	0	**1**	**1**	0	0	1550	2	4	256	8.5502×10^{-6}	0.1105
1	0	**1.5**	**1.5**	0	0	1550	2	4	256	0.0045	0.0802
1	0	**2**	**2**	0	0	1550	2	4	256	0.0487	0.1381

Table B.14 Cos-Gaussian beam received intensity differences according to beam waist

A_{c1}	A_{c2}	W_{s1}	W_{s2}	D_1	D_2	λ	L	m_f	N	DFA	DCA
0.5	-0.5	**0.5**	**0.5**	200j	-200j	1550	2	4	256	9.8421	0.9410
0.5	-0.5	**0.75**	**0.75**	200j	-200j	1550	2	4	256	0.7127	0.7448
0.5	-0.5	**1**	**1**	200j	-200j	1550	2	4	256	0.0481	1.1669
0.5	-0.5	**1.5**	**1.5**	200j	-200j	1550	2	4	256	0.0102	1.1383
0.5	-0.5	**2**	**2**	200j	-200j	1550	2	4	256	0.1035	1.1335

Table B.15 Cosh-Gaussian beam received intensity differences according to beam waist

A_{c1}	A_{c2}	W_{s1}	W_{s2}	D_1	D_2	λ	L	m_f	N	DFA	DCA
0.5	0.5	**0.5**	**0.5**	200	-200	1550	2	4	256	0.2814	0.3828
0.5	0.5	**0.75**	**0.75**	200	-200	1550	2	4	256	0.0018	0.2526
0.5	0.5	**1**	**1**	200	-200	1550	2	4	256	0.0134	0.4084
0.5	0.5	**1.5**	**1.5**	200	-200	1550	2	4	256	NaN	NaN
0.5	0.5	**2**	**2**	200	-200	1550	2	4	256	NaN	NaN

Table B.16 Sine-Gaussian beam received intensity differences according to beam waist

A_{c1}	A_{c2}	W_{s1}	W_{s2}	D_1	D_2	λ	L	m_f	N	DFA	DCA
0.5j	-0.5j	**0.5**	**0.5**	200j	-200j	1550	2	4	256	9.4294	1.3328
0.5j	-0.5j	**0.75**	**0.75**	200j	-200j	1550	2	4	256	0.7124	0.7396
0.5j	-0.5j	**1**	**1**	200j	-200j	1550	2	4	256	0.0483	1.1671
0.5j	-0.5j	**1.5**	**1.5**	200j	-200j	1550	2	4	256	0.0102	1.1385
0.5j	-0.5j	**2**	**2**	200j	-200j	1550	2	4	256	0.1034	1.1367

Table B.17 Sinh-Gaussian beam received intensity differences according to beam waist

A_{c1}	A_{c2}	W_{s1}	W_{s2}	D_1	D_2	λ	L	m_f	N	DFA	DCA
0.5	-0.5	**0.5**	**0.5**	-200	200	1550	2	4	256	0.8249	1.1519
0.5	-0.5	**0.75**	**0.75**	-200	200	1550	2	4	256	0.0028	0.3334
0.5	-0.5	**1**	**1**	-200	200	1550	2	4	256	0.0172	0.4981
0.5	-0.5	**1.5**	**1.5**	-200	200	1550	2	4	256	NaN	NaN
0.5	-0.5	**2**	**2**	-200	200	1550	2	4	256	NaN	NaN

Table B.18Annular Gaussian beam received intensity differences according to beam waist

A_{c1}	A_{c2}	W_{s1}	W_{s2}	D_1	D_2	λ	L	m_f	N	DFA	DCA
0.5	-0.5	**0.5**	**0.25**	0	0	1550	2	4	256	4.1069	0.4743
0.5	-0.5	**0.75**	**0.375**	0	0	1550	2	4	256	0.5990	0.1538
0.5	-0.5	**1**	**0.5**	0	0	1550	2	4	256	0.0788	0.1416
0.5	-0.5	**1.5**	**0.75**	0	0	1550	2	4	256	0.0058	0.1720
0.5	-0.5	**2**	**1**	0	0	1550	2	4	256	0.0606	0.2116

Received Field Tables According to Propagation Distance and Related Multiplying factor

Table B.19 Gaussian beam received intensity differences according to Distance and related multiplying factor

A_{c1}	A_{c2}	W_{s1}	W_{s2}	D_1	D_2	λ	L	m_f	N	DFA	DCA
1	0	1	1	0	0	1550	**0.1**	**1**	256	1.1882×10^{-6}	0.0121
1	0	1	1	0	0	1550	**0.2**	**1**	256	3.3623×10^{-6}	0.0286
1	0	1	1	0	0	1550	**0.5**	**1**	256	0.0011	0.1260
1	0	1	1	0	0	1550	**1**	**2**	256	14.072×10^{-6}	0.0968
1	0	1	1	0	0	1550	**2**	**4**	256	8.5502×10^{-6}	0.1105
1	0	1	1	0	0	1550	**5**	**10**	256	7.9428×10^{-6}	0.1144
1	0	1	1	0	0	1550	**10**	**20**	256	10.004×10^{-6}	0.1156
1	0	1	1	0	0	1550	**20**	**40**	256	10.170×10^{-6}	0.1162
1	0	1	1	0	0	1550	**50**	**100**	256	9.9743×10^{-6}	0.1166
1	0	1	1	0	0	1550	**100**	**200**	256	9.8605×10^{-6}	0.1167

Table B.20 Cos-Gaussian beam received intensity differences according to Distance and related multiplying factor

A_{c1}	A_{c2}	W_{s1}	W_{s2}	D_1	D_2	λ	L	m_f	N	DFA	DCA
0.5	-0.5	1	1	200j	-200j	1550	**0.1**	**1**	256	1.9299 x10^{-6}	0.0120
0.5	-0.5	1	1	200j	-200j	1550	**0.2**	**1**	256	18.330 x10^{-6}	0.0956
0.5	-0.5	1	1	200j	-200j	1550	**0.5**	**1**	256	0.4952	2.7852
0.5	-0.5	1	1	200j	-200j	1550	**1**	**2**	256	0.0893	1.6194
0.5	-0.5	1	1	200j	-200j	1550	**2**	**4**	256	0.0481	1.1669
0.5	-0.5	1	1	200j	-200j	1550	**5**	**10**	256	0.0396	0.9715
0.5	-0.5	1	1	200j	-200j	1550	**10**	**20**	256	0.0385	0.9185
0.5	-0.5	1	1	200j	-200j	1550	**20**	**40**	256	0.0382	0.8941
0.5	-0.5	1	1	200j	-200j	1550	**50**	**100**	256	0.0381	0.8802
0.5	-0.5	1	1	200j	-200j	1550	**100**	**200**	256	0.0381	0.8757

Table B.21 Cosh-Gaussian beam received intensity differences according to Distance and related multiplying factor

A_{c1}	A_{c2}	W_{s1}	W_{s2}	D_1	D_2	λ	L	m_f	N	DFA	DCA
0.5	0.5	1	1	200	-200	1550	**0.1**	**1**	256	0.0158	0.0505
0.5	0.5	1	1	200	-200	1550	**0.2**	**1**	256	0.0250	0.1202
0.5	0.5	1	1	200	-200	1550	**0.5**	**1**	256	0.2604	1.0339
0.5	0.5	1	1	200	-200	1550	**1**	**2**	256	0.0365	0.8285
0.5	0.5	1	1	200	-200	1550	**2**	**4**	256	0.0134	0.4084
0.5	0.5	1	1	200	-200	1550	**5**	**10**	256	0.0087	0.3180
0.5	0.5	1	1	200	-200	1550	**10**	**20**	256	0.0098	0.3049
0.5	0.5	1	1	200	-200	1550	**20**	**40**	256	0.0103	0.3007
0.5	0.5	1	1	200	-200	1550	**50**	**100**	256	0.0104	0.2989
0.5	0.5	1	1	200	-200	1550	**100**	**200**	256	0.0104	0.2984

Table B.22 Sine-Gaussian beam received intensity differences according to Distance and
related multiplying factor

A_{c1}	A_{c2}	W_{s1}	W_{s2}	D_1	D_2	λ	L	m_f	N	DFA	DCA
0.5j	-0.5j	1	1	-200j	200j	1550	**0.1**	**1**	256	2.2375×10^{-6}	0.0141
0.5j	-0.5j	1	1	-200j	200j	1550	**0.2**	**1**	256	0.5041	2.7831
0.5j	-0.5j	1	1	-200j	200j	1550	**0.5**	**1**	256	0.5041	2.7831
0.5j	-0.5j	1	1	-200j	200j	1550	**1**	**2**	256	0.0903	1.6176
0.5j	-0.5j	1	1	-200j	200j	1550	**2**	**4**	256	0.0483	1.1671
0.5j	-0.5j	1	1	-200j	200j	1550	**5**	**10**	256	0.0396	0.9742
0.5j	-0.5j	1	1	-200j	200j	1550	**10**	**20**	256	0.0384	0.9224
0.5j	-0.5j	1	1	-200j	200j	1550	**20**	**40**	256	0.0381	0.8987
0.5j	-0.5j	1	1	-200j	200j	1550	**50**	**100**	256	0.0380	0.8851
0.5j	-0.5j	1	1	-200j	200j	1550	**100**	**200**	256	0.0380	0.8807

Table B.23 Sinh-Gaussian beam received intensity differences according to Distance and
related multiplying factor

A_{c1}	A_{c2}	W_{s1}	W_{s2}	D_1	D_2	λ	L	m_f	N	DFA	DCA
0.5	-0.5	1	1	-200	200	1550	**0.1**	**1**	256	0.0360	0.0159
0.5	-0.5	1	1	-200	200	1550	**0.2**	**1**	256	0.0246	0.0731
0.5	-0.5	1	1	-200	200	1550	**0.5**	**1**	256	0.2435	0.6502
0.5	-0.5	1	1	-200	200	1550	**1**	**2**	256	0.0325	0.7245
0.5	-0.5	1	1	-200	200	1550	**2**	**4**	256	0.0172	0.4981
0.5	-0.5	1	1	-200	200	1550	**5**	**10**	256	0.0109	0.4098
0.5	-0.5	1	1	-200	200	1550	**10**	**20**	256	0.0131	0.3968
0.5	-0.5	1	1	-200	200	1550	**20**	**40**	256	0.0139	0.3930
0.5	-0.5	1	1	-200	200	1550	**50**	**100**	256	0.0142	0.3911
0.5	-0.5	1	1	-200	200	1550	**100**	**200**	256	0.0143	0.3905

Table B.24Annular Gaussian beam received intensity differences according to Distance and related multiplying factor

A_{c1}	A_{c2}	W_{s1}	W_{s2}	D_1	D_2	λ	L	m_f	N	DFA	DCA
0.5	-0.5	2	1	0	0	1550	**0.1**	**1**	256	0.1419	1.0331
0.5	-0.5	2	1	0	0	1550	**0.2**	**1**	256	5.4615 $\times 10^{-6}$	0.0333
0.5	-0.5	2	1	0	0	1550	**0.5**	**1**	256	0.7270	1.1485
0.5	-0.5	2	1	0	0	1550	**1**	**2**	256	0.1105	0.2867
0.5	-0.5	2	1	0	0	1550	**2**	**4**	256	0.0606	0.2116
0.5	-0.5	2	1	0	0	1550	**5**	**10**	256	0.0322	0.1344
0.5	-0.5	2	1	0	0	1550	**10**	**20**	256	0.0734	0.1260
0.5	-0.5	2	1	0	0	1550	**20**	**40**	256	0.0732	0.1247
0.5	-0.5	2	1	0	0	1550	**50**	**100**	256	0.0732	0.1240
0.5	-0.5	2	1	0	0	1550	**100**	**200**	256	0.0732	0.1238

APPENDIX C

CURRICULUM VITAE

PERSONAL INFORMATION

Surname, Name: ÇATMAKAŞ,Ömer Kemal

Nationality: Turkish (TC)

Date and Place of Birth: 27 February 1987, Diyarbakır

Marital Status: Single

Phone: 0506 405 77 77

email: omercatmakas@cankaya.edu.tr

EDUCATION

Degree	Institution	Year of Graduation
MS	Çankaya University Electronic and Communication Engineering	2014
BS	Çankaya University Electronic and Communication Engineering	2010
High School	Özel Yeni Ortadoğu Koleji	2004

WORK EXPERIENCE

Year	Place	Enrollment
2012- Present	Çankya Univ.	Specialist
2010-2012	ZTE	Technical Engineer

FOREIGN LANGUAGES

Advanced English, Elementary German

HOBBIES

Lomography, Computer Games, Playing Music, Kenpo.